Revealing the Incorporation of Cerium in Fluorapatite

Alain Manceau, Olivier Mathon, Kirill A Lomachenko, Mauro Rovezzi, Kristina O Kvashnina, Marie-Christine Boiron, Romain Brossier, Stephan N Steinmann

Revealing the incorporation of cerium in fluorapatite

Alain Manceau*[1,2], Olivier Mathon[1], Kirill A. Lomachenko[1], Mauro Rovezzi[3], Kristina O. Kvashnina[4,5], Marie-Christine Boiron[6], Romain Brossier[7], and Stephan N. Steinmann*[2]

[1]European Synchrotron Radiation Facility (ESRF), 38000 Grenoble, France
[2]ENS de Lyon, CNRS, Laboratoire de Chimie, 69342 Lyon, France
[3]Université Grenoble Alpes, CNRS, OSUG, FAME, 38000 Grenoble, France
[4]The Rossendorf Beamline, ESRF, F-38000 Grenoble, France
[5]Helmholtz Zentrum Dresden-Rossendorf (HZDR), Institute of Resource Ecology, 01314 Dresden, Germany
[6]Univ. Lorraine, ENSG, CNRS, GeoRessources Lab, 54000 Nancy, France
[7]Université Grenoble Alpes, CNRS, ISTerre, 38000 Grenoble, France

Corresponding authors: alain.manceau@ens-lyon.fr; stephan.steinmann@ens-lyon.fr

Keywords: Apatite, Durango, Imilchil, EXAFS, HERFD-EXAFS, DFT, VASP

ABSTRACT

Fluorapatite (FAp, nominally $Ca_5(PO_4)_3F$) is the most common phosphate mineral at the Earth's surface and a main host for rare earth elements (REE) in magmatic and hydrothermal ore deposits and in marine sediments. Our understanding of the enrichment process of REE in FAp rests upon two foundations: (1) being able to elucidate the thermodynamic driving force for their partitioning between the Ca1 and Ca2 structural sites, and (2) being able to determine how the substitution of REE(III) for Ca(II) is charge compensated. A main unsolved question is the marked preference of the larger light REE (lanthanum → samarium) for the smaller Ca2 site. We used density functional theory (DFT) and high-energy resolution fluorescence-detected extended X-ray absorption fine structure (HERFD-EXAFS) spectroscopy to gain detailed insight into the bonding energy, electronic structure, and short-range order of cerium (Ce) in natural FAp. Results show that Ce(III) has a marked preference for a Ca2 site where the nearest five-valent phosphorous cation is replaced with a tetravalent silicon cation, thus balancing the charge excess of the Ce impurity locally. Atomic charge calculations show that the Ca2 site is more ionic than the Ca1 site and that the energetics of the site preference is linearly correlated to the ionization energy of the substituent. Cations with a low energy

of ionization, like Ce, preferably occupy the Ca2 site. Novel combination of HERFD-EXAFS spectroscopy and DFT appears to be the most straightforward and reliable way to assess the crystal chemistry of trace elements in compositionally complex natural materials, and opens a previously unavailable avenue for mechanistic investigation of metal enrichment in ore deposits.

INTRODUCTION

FAp widely occurs in calcium-rich igneous rocks[1,2] and as biogenic remain in ancient (e.g., phosphorite)[3–7] and modern (e.g., deep-sea mud) marine deposits.[8–12] The crystal structure of FAp permits a wide range of cation and anion substitutions.[13–18] In particular, it has two calcium sites, a larger Ca1 site surrounded by 6 + 3 oxygen and a smaller Ca2 site surrounded by 6 oxygen and one fluorine,[19,20] which can accommodate monovalent, divalent, and trivalent cations as substituents, such as Na, Sr, Cd, and rare-earth elements of the lanthanide series (REE) and yttrium (REY).[8–12,21–25] Igneous and sedimentary fluorapatites commonly contain ore grades of several percent (w/w) REY.[9,26–29,12,30,31] REY enrichment occurs in contact with magmatic and hydrothermal fluids for igneous FAp,[30,32–34] and in contact with bottom seawaters and pore waters for detrital biogenic FAp.[11,35–37]

In addition to having a different size, the Ca1 and Ca2 sites also differ in their exposure to fluids. The crystal framework of apatite consists of face-shared Ca1 octahedra linked through oxygen atoms shared with PO_4 tetrahedra (Figure 1a).[19,20] The Ca1-PO_4 framework circumscribes one-directional tunnels along the *c* axis demarcated by CaO_6F polyhedra (Ca2 site) on the walls that are in contact with circulating solutions in the lumen of the tunnels and along the external surfaces of the mineral grains. The distribution of REE between the two Ca sites of FAp has been addressed in many studies performed on natural and synthetic minerals.[19,38–46] REE prefer the Ca2 site over the Ca1 site with a Ca2/Ca1 site occupancy ratio that decreases from light (LREE) to heavy (HREE) REE. Site preference in FAp has been rationalized variously in terms of ionic radii of REE(III) and Ca(II), equalization of Ca1, Ca2, and F bond valences, bond covalencies, and minimization of strain effects.[40–43,46–48] Still, no satisfactory explanation has been offered to support the preference of LREE with a radius larger than Ca(II) for the smaller Ca2 site.

An estimated Ca2/Ca1 occupancy ratio of 3.67 has been estimated for Ce in singly-REE substituted synthetic FAp by Fleet and Pan in 1995 using single-crystal X-ray diffraction.[42] As comprehensive as this study is, Feet and Pan further noted in 1997 that “quantitative transference of laboratory REE site preferences to natural apatites is frustrated by the compositional complexity in nature”.[43] Crystallographic data on natural apatites indeed provide site occupancies averaged over all

substituents, and therefore lack structural sensitivity to specific REE. The site occupancy of a given REE can be apprised in principle by extended X-ray absorption fine structure (EXAFS) spectroscopy as this technique is element selective. However, a major roadblock in analyzing multi-elemental Earth materials by EXAFS is the overlap of the X-ray fluorescence lines from two or more elements,[8,49,50] and therefore its application to REE-containing natural apatites is unprecedented.

Another key question in understanding the uptake of REY into FAp is how the increase of positive electronic charge resulting from the REE(III) for Ca(II) substitution is compensated chemically. Two coupled substitutions have been proposed: REE(III) + Na^{+} ↔ 2Ca(II) and REE(III) + Si^{4+} ↔ P^{5+} + Ca(II).[39–43,46] X-ray refinement of singly La, Nd, Gd, and Dy substituted synthetic FAp found that Na occupies the Ca1 site[42,46] (Na1), and that charge balance is maintained with both Na and Si (Na > Si).[46] Atomistic calculation of the formation enthalpy of $Ca_9Nd(PO_4)_5SiO_4F_2$ and $Ca_8NdNa(PO_4)_6F_2$ showed that the first compound is thermodynamically more stable than the second, and therefore that the heterovalent REE(III) - Ca(II) substitution is more likely charge balanced by parallel Si^{4+} ↔ P^{5+} substitution than by Na^{+} ↔ Ca^{2+} substitution,[47] at odds with diffraction results.[46] Still, the theoretical study confirmed the preference of Na for the Ca1 site and of Nd for the Ca2 site, and predicted that the Nd-Si coupled substitution takes place at short distance in the FAp structure.

Despite the large amount of literature available on REE-containing FAp, several questions and ambiguities on the atomic-scale structure of this common phosphate mineral remain. Although LREE most likely occupy the Ca2 site in natural FAp, direct confirmation by EXAFS spectroscopy is clearly desirable. Here, the complication arising from the multi-elemental nature of natural FAp was circumvented by filtering the unwanted X-ray fluorescence lines with analyzer crystals in high energy resolution fluorescence detection mode (HERFD-EXAFS).[51–53,50] The nature of the charge compensating cation and the energetic driving force for the site preference of REE remain unresolved. The two questions were addressed theoretically by optimizing the geometries and calculating the total energies of (1) Na/Si charge-compensated Ce(III)-FAp models, and (2) Mg(II), Sr(II), Ba(II), and Cd(II)-substituted FAp models. The choice of Ce as REE was dictated because of its broad interest in earth science aiming at inferring magmatic and marine sediment processes, and paleo-redox and paleo-environmental reconstructions.[8,36,54–60] For the sake of convenience, we will start by presenting the quantum-mechanical results. The geometrically-optimized structures will be used next to interpret the Ce-EXAFS data.

MATERIALS AND METHODS

DTF. Density functional theory (DFT) computations were performed in the Vienna Ab-initio Simulation Package (VASP) software.[61,62] The projector augmented wave (PAW) pseudopotentials[63,64] were used for the core-electron interaction, in combination with a converged energy cutoff of 500 eV for the planewave basis set. The energies and forces were evaluated at the generalized gradient approximation (GGA) with a Perdew-Burke-Ernzerhof (PBE)[65] exchange-correlation functional in conjunction with the density-dependent dispersion correction dDsC.[66,67] The Brillouin zone of 2 x 2 x 2 supercells with stoichiometry $Ca_{80}P_{48}O_{192}F_{16}$ (FAp has two formula units in the primitive cell) and cell vector lengths of about 18.8 Å and 13.7 Å for in-plane and out-of-plane directions was probed at the Gamma point. A Fermi-smearing of 0.026 eV (~300 K) was applied, but had no impact on the electronic energy for this insulating material. During the self-consistent field procedure, the wave functions were optimized to an energy-change below 10^{-6} eV. The numerical settings for the fast Fourier transform grids was set to "accurate" and the real-space projector operators were determined via the recommended automatic optimization scheme. For geometry optimizations all atoms and the unit cell were fully relaxed until the maximum force was below 0.05 eV/Å. The atomic Hirshfeld charges, which are known to depend little on the electronic structure and the basis set and are well suited for assessing charge-transfers,[68] have been taken from the standard output of the dDsC dispersion correction. The maximum error in the interatomic distances of FAp calculated with VASP relative to the diffraction values[19] is 1.15% (Table S1).

Samples and EXAFS Spectroscopy. Two magmatic-hydrothermal FAp were studied by EXAFS spectroscopy, one from Cerro de Mercado near Durango, Mexico,[69] and another from Imilchil, Morocco.[70–72] The Durango FAp was characterized previously by laser ablation inductively coupled plasma mass spectrometry (LA-ICP-MS) and electron probe microanalysis (EPMA).[8] It contains 4,890 mg/kg (ppm) Ce, 3,340 mg/kg La, and 971 mg/kg Pr. The chemical composition of the Imilchil FAp is reported in Table S2. It contains 4,864 mg/kg (ppm) Ce, 2,678 mg/kg La, and 492 mg/kg Pr. The Ce L_3-edge (5723 eV) HERFD-EXAFS spectra were measured at the European Synchrotron Radiation Facility (ESRF), at room temperature on ID24-DCM and at 8-12 K on FAME-UHD (BM16) for the Durango FAp, and at room temperature on BM20 for the Imilchil FAp. No changes in spectral features were noted during the courses of data collection that would indicate radiation damage. Experimental details are provided in the Supporting Information (SI).

The benefits of HERFD-EXAFS are shown in Figure 2. First, a spectrometer acts both as a low-pass and high-pass filter, eliminating (1) the undesired fluorescence lines at lower and higher energies than that of the Ce $L_{\alpha 1}$ line at 4839 eV, here the $L_{\alpha 1+2}$ (~4647 eV) and $L_{\beta 1}$ (~5038 eV) lines of La and the $L_{\alpha 1+2}$ (~5035 eV) of Pr, and (2) the elastic and inelastic rays at higher energy (Figure

2a). As a result, the background signal is lower, and therefore the signal/noise ratio higher and the detection limit lower (Figure 2b). Second, filtering the Ce $L_{\alpha 1}$ line allows extending the *k*-range of EXAFS beyond the La L_2-edge at 5891 eV and the Pr L_3-edge at 5964 eV (Figure 2b). This phenomenon was first observed in 2005 for La in LaOCL.[73]

RESULTS AND DISCUSSION

DFT. The first series of calculation focuses on the site preference of Na when Ce occupies the Ca1 site (Ce1) or the Ca2 site (Ce2) site (see polyhedral drawings in Figure 3). This was accomplished by calculating the energy difference of models Ce1-Na1-close and Ce1-Na2-close, on one hand, and Ce2-Na1-close and Ce2-Na2-close, on the other hand, in which Na is positioned in closest proximity to Ce to balance locally the excess of positive charge resulting from the Ce(III) for Ca(II) substitution. Na in the Ce2 site (Na2) is less favorable than in the Ce1 site (Na1) by -0.30 eV/cell when Ce is in the Ca1 site and by -0.18 eV/cell when Ce is in the Ca2 site (Table 1). Na clearly prefers the Ca1 site, in agreement with the structural refinement of synthetic FAp using X-ray diffraction.[42,46] Therefore, Na will be placed in this site in all further calculations. Next, we interrogated the site preference of Ce when the charge excess is compensated by Na (Ce1-Na1-close and Ce2-Na1-close models) or by Si (Ce1-Si-close and Ce2-Si-close models). The Ce1-Na1-close and Ce2-Na1-close models have the same total energy, whereas the Ce2-Si-close model is -0.08 eV/cell lower in energy than the Ce1-Si-close model (Table 1). The finding predicts that Ce prefers the Ca2 site when the charge is balanced by Si, otherwise Ce has no preference when the charge is balanced by Na.

The question that remains to handle is which of the Na or Si substituents provides the lowest energy structure. The answer was obtained from the energy difference between models with the compensating Na and Si cations placed either in closest proximity or far away from Ce (d > 9 Å). Configurations that promote local charge balance are always the most energetically competitive structures (Table 1). The gain in energy obtained with the Na short-range surrounding of Ce is -0.09 eV/cell for Ce2-Na1-close and -0.18 eV/cell for Ce1-Na1-close. With Si, the gains are -0.36 eV/cell for Ce2-Si-close and -0.34 eV/cell for Ce1-Si-close. This result shows that the Ce(III) substitution is better charge compensated by Si than by Na, regardless of the site occupancy of Ce. However, given that the Ce2-Si-close model is 0.08 eV/cell more stable than the Ce1-Si-close model, we conclude that Ce substitutes into the Ca2 site with a Si atom next to it at thermodynamic equilibrium.

To be examined now is whether the reason for the Ca2-Si preference is structural or electronic. In FAp, each apex of a $Ca1O_6$ octahedron shares one oxygen with a PO_4 tetrahedron (corner-sharing

linkage), whereas four apices of the $Ca2O_6F$ polyhedron share one oxygen with a PO_4 tetrahedron (corner-sharing linkage) and two apices share their oxygen atoms with a single PO_4 tetrahedron (edge-sharing linkage, Figure 1b). The Ca2-P distance is 3.07 Å across the shared edge and 3.26-3.68 Å across the shared apices. The most favorable configuration from an energetic standpoint is that in which the nearest P atom is replaced with a Si atom, yielding a Ce2-Si distance of 3.09 Å (Ce2-Si-close model, Figure 3a).

Examination of the Ce1-Si-close atomic arrangement shows that one of the three second-nearest O atoms of the Ca1 site at 2.81 Å and bonded to P (1.53 Å) and Ca2 (2.35 Å) in FAp,[19] bonds also the Ce1 atom at 2.54 Å in the optimized structure. The Ce1 coordination is 7 + 2, instead of 6 + 3 for Ca1 in FAp (Figure 3b). Interestingly, the displaced O atom is the one bonded to Si in Ce1-Si-close, instead of P in FAp. As a result of the O displacement, the SiO_4 tetrahedron shares an edge, and not an apice, with the $Ce1O_7$ polyhedron at a Ce-Si distance of 3.16 Å (Figures 1b and 3). The relaxation of the atomic positions around the substitutional Ce1 atom allows local balancing of the charge excess of the Ce1 site similarly to the Ce2 site. The charge compensating Si atom is 3.16 - 3.09 = 0.07 Å closer to Ce in the Ca2 site than in the Ca1 site. It is difficult to assess if the reduction in distance is sufficient to account for the 0.08 eV/cell gain in thermodynamic stability for the Ce2 partitioning relative to the Ce1 partitioning (Table 1). Compelling evidence for electronic effects on site preference is presented next.

Electronic effects were addressed with considerations of four divalent Me(II) substituents: Mg(II), Cd(II), Sr(II), and Ba(II). The first parameter examined is the cation size, reasoning that cations smaller than Ca (1.00 Å) should substitute into the smaller Ca2 site (<d(Ca-O)> = 2.40 Å for the six-fold coordination) and larger cations should substitute into the larger Ca1 site (<d(Ca-O)> = 2.43 Å for the six-fold coordination).[19] A regression analysis of the effective ionic radius[74] of the Me(II) substituents against the difference of total energy between the two Ca sites (E(Me2) – E(Me1), Table S3) shows moderate correlation (R^2 = 0.79, Figure 4a). Furthermore, the Ce2-Si-close model, and to a lesser extent the Ce1-Na-close/Ce2-Na-close models, are distant from the regression line.

Besides their size difference, another distinction of the Ca1 and Ca2 sites is their ionicity. Calculation of atomic charges shows that Ca has a charge of 0.429e in the Ca1 site and 0.475e in the Ca2 site, indicating that the Ca2 site has a higher ionic character. Therefore, we sought whether a correlation existed between the atomic charge and the site preference of the four Me(II) cations (Table S3). Figure 4b shows that the two variables are strongly correlated (R^2 = 0.92): the higher the difference of atomic charge of a Me(II) cation between the Ca2 and Ca1 sites, the higher is its preference for the Ca2 site, in line with the higher ionicity of the Ca2 site of FAp. The relationship

between Me(II) partitioning and ionicity of the Ca site is further supported by the fact that Ca is close to the regression line, as this atom was not considered in the linear fit. The Ce2-Si-close and the Ce1-Na-close/Ce2-Na-close models are far apart from the regression line due to the formal trivalent charge of Ce(III) (Figure 4b, Table S4).

Which distinctive electronic property causes a Me(II) cation to acquire a specific atomic charge in a Ca site that eventually determines its affinity for this site? What immediately comes to mind is its ionization energies. Figures 4c and 4d show that the first and second ionization energies are linearly correlated to E(Me2) - E(Me1) (R^2 = 0.90 and 0.93), thereby backing up our hypothesis. Remarkably, the Ce(III) cation from the Ce2-Si-close model is close to the two regression lines, which indicates that this cation is energetically and electronically well stabilized in the Ca2 site. This finding suggests that ionization energy is the main thermodynamic driving force for the partitioning of Ce(III) among the Ca1 and Ca2 sites in FAp, rather than the 0.07 Å difference in the Ce-Si interatomic distances between the two sites.

EXAFS Spectroscopy. The EXAFS spectra and Fourier transforms (FT) of the Durango FAp measured at room and low temperature (Durango-RT, Durango-HeT) and of the Imilchil FAp measured at room temperature (Imilchil-RT) are presented in Figure 5. The Durango spectrum has a higher amplitude at HeT, which is reflected in the FT by a considerable enhancement of the second and third peaks attributed to the dominant contribution of the Ce-P and Ce-Ca atomic pairs (Figure 3). The thermal motion of the Ce-P and Ce-Ca pairs is much more pronounced than that of the Ce-O pair at shorter bond distance (1st FT peak). Comparing the imaginary parts of the FT (i.e., oscillatory curves on Figure 5b), we find that they are superimposed at RT and HeT, which excludes a temperature-dependence of the bond distances. Thus, the Ce-P and Ce-Ca motions are harmonic with respect to the equilibrium position of the Ce, P, and Ca atoms. Large temperature-dependence of the cation shells has been observed previously for the Mn-Mn and Pb-Mn pairs in phyllomanganates,[75,76] but the physical motion was anharmonic, perhaps as a result of the layered structure of phyllomanganates and the implication of the two-dimensionality on atomic vibrational modes. The Durango-RT and Imilchil-RT spectra and FT are much alike in their amplitude and phase, indicating that Ce has similar bonding environment in the two FAp (Figure 5c,d). The site occupancy of Ce and the charge compensation mechanism are examined next with the better quality Durango-RT data.

Apatite is chemically simple, comprising only two cations, Ca and P, yet its structure is complex with two Ca sites, each surrounded by several and partly overlapping P and Ca shells between 3.0 Å and 4.1 Å (Figure 3). Least-squares fitting the average distances and coordination numbers (*CN*) of the 4-5 nearest O, P, and Ca shells around Ce, and the mean-square displacement of the constitutive

atoms in each of them (Debye-Waller term, σ), gives multiple optima in the parameter space. Additional complications arise from multiple scattering events of the photoelectron that are not negligible at $R_{eff} \geq 3.6$ Å, where R_{eff} is the half-path length of the scattering path (Figure S1). It is critical not to overparametrize any of the models tested, and good quality fits that are both statistically robust and structurally meaningful are difficult to obtain. In our hands, only the average distance of the first Ce-O shell can be obtained reliably, and can be used to distinguish unequivocally between the Ce1 and the Ce2 sites. In the DFT model, the 9 O atoms of the Ce1 site are at 2.549 Å on average (σ = 0.078 Å) and the 6 nearest O atoms of the Ce2 site are at 2.428 Å on average (σ = 0.035 Å) (Figure 3). The best-fit EXAFS distance is 2.43 Å, identical to the DFT Ce2-O distance. Best-fit coordination numbers are highly correlated to σ, and therefore do not yield reliable results. In addition, the distribution of Ce-O distances is asymmetric in the lowest energy Ce2-Si-close model (Figure 3b), and its EXAFS analysis using a standard Gaussian-type distribution of interatomic distances will exclude its full distribution and lose O atoms ($CN_{eff} < CN_{str}$).

A holistic alternative to determination of the bonding environment of Ce in apatite consists of comparing data with DFT-derived EXAFS models. The EXAFS spectra of five lowest energy DFT structures were generated using the FEFF 8.2 code.[77] The degree to which a theoretical spectrum resembles the Durango-RT FAp spectrum was evaluated with the normalized sum-of-squares ($NSS = \sum(k^2\chi_{exp} - k^2\chi_{fit})^2/\sum(k^2\chi_{exp})^2$) parameter.

The theoretical Ce2-Si-close and Ce1-Si-close spectra and FT are compared to the Durango-RT data in Figure 6. The Ce2-Si-close model well replicates the phase and amplitude of the experimental wave and FT (Figure 6a,b, $NSS = 0.05$). This good match was obtained by optimizing only six EXAFS parameters: the threshold Fermi level of the photoelectron ($\Delta E = (k/0.512)^2$) for the wave phase, four Debye-Waller (DB) values for single-scattering events between the central atom (Ce) and the O, P1, P2, and Ca shells up to 4.15 Å (Figure 3b), and one DB value for multiple scattering (MS) events (σ(O) = 0.12 Å, σ(Si,P1) = 0.07 Å, σ(P2) = 0.12 Å, σ(Ca) = 0.11 Å, σ(MS) = 0.17 Å). Lower DB values for the cation shells were obtained with Durango-HeT (σ(P1) = 0.04 Å, σ(P2) = 0.09 Å, σ(Ca) = 0.08 Å), consistent with the reduction of atomic motion at low temperature. In contrast to Ce2-Si-close, Ce1-Si-close failed to replicate the experimental wave phase and amplitude, yielding considerable disparity between measurement and prediction ($NSS = 0.30$) (Figure 6c,d). The theoretical wave is shifted to lower wavevector values (k) in the 3.0-6.0 $Å^{-1}$ k-range, and this displacement can be used to estimate the maximum amount, or detection limit, of Ce in the Ca1 site.

The Ce1 component makes up <10% of Ce total, on the basis of linear-combinations of the Ce1-Si-close and Ce2-Si-close spectra.

EXAFS ordinarily fails to distinguish between P and Si atomic neighbors for their photoelectron scattering amplitudes are similar (Z = 15 and 14), and it has little sensitivity to the Na shell at d = 3.46 Å (Ce1-Na1-close) and 3.98 Å (Ce2-Na1-close, distance histograms of Figures S3a, S4a). Therefore, the Ce-Na and Ce-Si models are virtually impossible to differentiate with the usual shell-by-shell least-squares fitting analysis. Using a whole-structure approach, like here, allows differentiation of the two models, because the Si for P, and the Na for Ca, substitutions modify more than just two discrete atomic shells, but a larger portion of the short and medium range orders around the Ce impurity. Si for P distinction is illustrated in Figure S2 with the poorer match to data of Ce2-Si-far (*NSS* = 0.06) than Ce2-Si-close (*NSS* = 0.05), indicating that the Ce(III) for Ca substitution is paired with a Si for P substitution at short distance in the apatite structure. Ce2-Si-far has longer Ca-Ca pairs than Ce2-Si-close (histograms of Figures 3b and S2a), which are seen in the FT of Ce2-Si-far by a shift to longer distance of the Ce-Ca peak (Figure S2c). Similarly, Ce2-Na1-close (*NSS* = 0.08) and Ce1-Na1-close (*NSS* = 0.28) have EXAFS and FT features that differentiate them from other models (Figures S3b,c and S4b,c).

CONCLUDING REMARKS

The results of this study lead us to revisit a previous suggestion that the distribution of a substituent between the Ca1 and Ca2 sites is a marker for the enrichment mechanism, which distinguishes secondary diffusion process through ion-exchange from authigenic precipitation or recrystallization.[78] The idea was proposed after a study on the incorporation of Cd in sedimentary FAp using EXAFS spectroscopy.[22] It was found that Cd occupied the Ca2 site in the sedimentary FAp and was substituted in the Ca1 site in a synthetic Cd-doped hydrothermal reference. It was hypothesized that the Cd enrichment in conditions of the Earth's surface occurred by a diffusion mechanism into the apatite nanopores or along the external surfaces of the mineral grains, because the Ca2 sites are exposed to circulating fluids (Figure 1a). An authigenic formation process was discounted. This hypothesis is supported here and in the DFT study of Tamm and Peld[79] by the energetic preference of Cd for the Ca1 site (Figure 4). Thus, substitution of Cd in the Ca2 site of the natural sedimentary FAp was metastable and, consequently, the site occupancy of Cd had registered the geochemical process that the FAp had undergone. Figure 4 shows that Mg may also be used as a structural probe for past geochemical processes, whereas Ce clearly cannot.

This study presents the first demonstration that Ce(III) is incorporated in the Ca2 site of natural magmatic/hydrothermal FAp and shows that the excess of positive charge resulting from the Ce(III) for Ca(II) substitution is balanced by a Si for P substitution at short distance. It remains to be seen whether this finding can be extended to biogenic FAp, such as those occurring in marine sediments, which are prospective resources for REY.[80] Bioapatites from ocean-floor sediments have similar Ce L_3-edge X-ray absorption near-edge structure (XANES) spectra as magmatic/hydrothermal FAp,[8] indicating that Ce is also trivalent. But XANES spectroscopy does not inform on the chemical form of REY, and therefore on ore enrichment processes which can be different for high-temperature magmatic/hydrothermal and low-temperature sedimentary deposits. From a broader earth sciences perspective, the new analytical possibilities offered by the combination of HERFD-EXAFS and DFT is perhaps the most exciting finding of this work, as it opens up the possibility to differentiate metal enrichment by ion-exchange and precipitation process.

ASSOCIATED CONTENT

Supporting Information

EXAFS spectroscopy and LA-ICP-MS experimental methods, optimized (VASP) versus experimental (XRD) interatomic distances for FAp, total energies and atomic charges of the Me(II)-FAp models, atomic charges of the Ce-Si and Ce-Na models, chemical analysis of the Imilchil apatite, Cartesian coordinates of the Ce1-Na1-close, Ce2-Na1-close, Ce1-Si-close, Ce2-Si-close, and Ce2-Si-far models, EXAFS spectra (PDF).

ACKNOWLEDGEMENTS

The SOLEIL facility provided synchrotron beamtime via the French CRG program at ESRF (proposal #20210014). Financial support was provided by the European Research Council (ERC) under Advanced Grant DEEP-SEE (#101052913). Views and opinions expressed are, however, those of the authors only and do not necessarily reflect those of the European Union or the European Research Council. Neither the European Union nor the granting authority can be held responsible for them. LA-ICP-MS measurements at GeoRessources in Nancy were supported by the ANR (ANR-10-LABX-21-RESSOURCES21), the Région Lorraine, and the FEDER program from the European Community.

REFERENCES

(1) Harlov, D. E.; Rakovan, J. F. *Apatite: A Mineral for All Seasons*; Elements; 2015; Vol. 11.

(2) Nash, W. P. Phosphate Minerals in Terrestrial Igneous and Metamorphic Rocks. In *Phosphate Minerals*; Nriagu, J. O., Moore, P. B., Eds.; Springer-Verlag, 1984; p 442.

(3) Knudsen, A. C.; Gunter, M. E. Sedimentary Phosphorites - An Example: Phosphoria Formation, Southeastern Idaho, USA. In *Phosphates: Geochemical, Geobiological, and Materials Importance*; Kohn, M. J., Rakovan, J., Hughes, J. M., Eds.; Rev. Miner. Geochem.; 2002; Vol. 48, pp 363–389.

(4) Hein, J.; Koschinsky, A.; Mikesell, M.; Mizell, K.; Glenn, C.; Wood, R. Marine Phosphorites as Potential Resources for Heavy Rare Earth Elements and Yttrium. *Minerals* **2016**, *6*, n° 88.

(5) Xiqiang, L.; Hui, Z.; Yong, T.; Yunlong, L. REE Geochemical Characteristic of Apatite: Implications for Ore Genesis of the Zhijin Phosphorite. *Minerals* **2020**, *10*, n° 1012.

(6) Jiang, X.; Sun, X.; Chou, Y.; Hein, J.; He, G.; Fu, Y.; Li, D.; Liao, J.; Ren, J. Geochemistry and Origins of Carbonate Fluorapatite in Seamount Fe-Mn Crusts from the Pacific Ocean. *Mar. Geol.* **2020**, *423*, n° 106135.

(7) Valetich, M.; Zivak, D.; Spandler, C.; Degeling, H.; Grigorescu, M. REE Enrichment of Phosphorites: An Example of the Cambrian Georgina Basin of Australia. *Chem. Geol.* **2022**, *588*, n° 120654.

(8) Manceau, A.; Paul, S.; Simionovici, A.; Magnin, V.; Balvay, M.; Findling, N.; Rovezzi, M.; Muller, S.; Garbe-Schonberg, D.; Koschinsky, A. Fossil Bioapatites with Extremely High Concentrations of Rare Earth Elements and Yttrium from Deep-Sea Pelagic Sediments. *ACS Earth Space Chem.* **2022**, *6*, 2093–2103.

(9) Bi, D.; Shi, X.; Huang, M.; Yu, M.; Zhou, T.; Zhang, Y.; Zhu, A.; Shi, M.; Fang, X. Geochemical and Mineralogical Characteristics of Deep-Sea Sediments from the Western North Pacific Ocean: Constraints on the Enrichment Processes of Rare Earth Elements. *Ore Geol. Rev.* **2021**, *138*, n° 104318.

(10) Liao, J.; Chen, J.; Sun, X.; Wu, Z.; Deng, Y.; Shi, X.; Wang, Y.; Chen, Y.; Koschinsky, A. Quantifying the Controlling Mineral Phases of Rare-Earth Elements in Deep-Sea Pelagic Sediments. *Chem. Geol.* **2022**, *595*, n° 120792.

(11) Liao, J.; Sun, X.; Li, D.; Sa, R.; Lu, Y.; Lin, Z.; Xu, L.; Zhan, R.; Pan, Y.; Xu, H. New Insights into Nanostructure and Geochemistry of Bioapatite in REE-Rich Deep-Sea Sediments: LA-ICP-MS, TEM, and Z-Contrast Imaging Studies. *Chem. Geol.* **2019**, *512*, 58–68.

(12) Kon, Y.; Hoshino, M.; Sanematsu, K.; Morita, S.; Tsunematsu, M.; Okamoto, N.; Yano, N.; Tanaka, M.; Takagi, T. Geochemical Characteristics of Apatite in Heavy REE-Rich Deep-Sea Mud from Minami-Torishima Area, Southeastern Japan. *Res. Geol.* **2014**, *64*, 47–57.

(13) Leventouri, T.; Chakoumakos, B.; Moghaddam, H.; Perdikatsis, V. Powder Neutron Diffraction Studies of a Carbonate Fluorapatite. *J. Mater. Res.* **2000**, *15*, 511–517.

(14) Yi, H.; Balan, E.; Gervais, C.; Segalen, L.; Fayon, F.; Roche, D.; Person, A.; Morin, G.; Guillaumet, M.; Blanchard, M.; Lazzeri, M.; Babonneau, F. A Carbonate-Fluoride Defect Model for Carbonate-Rich Fluorapatite. *Am. Miner.* **2013**, *98*, 1066–1069.

(15) Hughes, J. M.; Pasteris, J. D. Environmental Mineralogy of Apatite. In *Phosphates: Geochemical, geobiological, and materials importance*; Harlov, D. E., Rakovan, J. F., Eds.; Elements; 2015; Vol. 11, pp 195–200.

(16) Kim, Y.; Konecke, B.; Fiege, A.; Simon, A.; Becker, U. An Ab-Initio Study of the Energetics and Geometry of Sulfide, Sulfite, and Sulfate Incorporation into Apatite: The Thermodynamic Basis for Using This System as an Oxybarometer. *Am. Miner.* **2017**, *102*, 1646–1656.

(17) Camara, F.; Curetti, N.; Benna, P.; Abdu, Y. A.; Hawthorne, F. C.; Ferraris, C. The Effect of Type-B Carbonate Content on the Elasticity of Fluorapatite. *Phys. Chem. Miner.* **2018**, *45*, 789–800.

(18) Kim, Y.; Konecke, B.; Simon, A.; Fiege, A.; Becker, U. An Ab-Initio Study on the Thermodynamics of Disulfide, Sulfide, and Bisulfide Incorporation into Apatite and the Development of a More Comprehensive Temperature, Pressure, PH, and Composition-Dependent Model for Ionic Substitution in Minerals. *Am. Miner.* **2022**, *107*, 1995–2007.

(19) Hughes, J. M.; Cameron, M.; Crowley, K. D. Structural Variations in Natural F, OH, and Cl Apatites. *Am. Miner.* **1989**, *74*, 870–876.

(20) Hughes, J. M.; Rakovan, J. The Crystal Structure of Apatite, $Ca_5(PO_4)_3(F,OH,Cl)$. In *Phosphates: Geochemical, Geobiological, and Materials Importance*; Kohn, M. J., Rakovan, J., Hughes, J. M., Eds.; Rev. Miner. Geochem.; 2002; Vol. 48, pp 1–12.

(21) Rakovan, J. F.; Hughes, J. M. Strontium in the Apatite Structure: Strontian Fluorapatite and Belovite-(Ce). *Can. Miner.* **2000**, *38*, 839–845.

(22) Sery, A.; Manceau, A.; Greaves, G. N. Chemical State of Cd in Apatite Phosphate Ores as Determined by EXAFS Spectroscopy. *Am. Miner.* **1996**, *81*, 864–873.

(23) Pan, Y.; Fleet, M. Compositions of the Apatite-Group Minerals: Substitution Mechanisms and Controlling Factors. In *Phosphates: Geochemical, Geobiological, and Materials Importance*; Kohn, M., Rakovan, J., Hughes, J., Eds.; 2002; Vol. 48, pp 13–49.

(24) Belousova, E. A.; Griffin, W. L.; O'Reilly, S. Y.; Fisher, N. I. Apatite as an Indicator Mineral for Mineral Exploration: Trace-Element Compositions and Their Relationship to Host Rock Type. *J. Geochem. Explor.* **2002**, *76*, 45–69.

(25) Frank-Kamenetskaya, O.; Rozhdestvenskaya, I.; Rosseeva, E.; Zhuravlev, A. Refinement of Apatite Atomic Structure of Albid Tissue of Late Devon Conodont. *Crystallogr. Rep.* **2014**, *59*, 41–47.

(26) Jaireth, S.; Hoatson, D. M.; Miezitis, Y. Geological Setting and Resources of the Major Rare-Earth-Element Deposits in Australia. *Ore Geol. Rev.* **2014**, *62*, 72–128.

(27) Li, X.; Zhou, M. Multiple Stages of Hydrothermal REE Remobilization Recorded in Fluorapatite in the Paleoproterozoic Yinachang Fe-Cu-(REE) Deposit, Southwest China. *Geochim. Cosmochim. Acta* **2015**, *166*, 53–73.

(28) Bodeving, S.; Jones, A.; Swinden, S. Carbonate-Silicate Melt Immiscibility, REE Mineralising Fluids, and the Evolution of the Lofdal Intrusive Suite, Namibia. *Lithos* **2017**, *268*, 383–398.

(29) Broom-Fendley, S.; Brady, A. E.; Wall, F.; Gunn, G.; Dawes, W. REE Minerals at the Songwe Hill Carbonatite, Malawi: HREE-Enrichment in Late-Stage Apatite. *Ore Geol. Rev.* **2017**, *81*, 23–41.

(30) Anenburg, M.; Mavrogenes, J.; Frigo, C.; Wall, F. Rare Earth Element Mobility in and around Carbonatites Controlled by Sodium, Potassium, and Silica. *Sci. Adv.* **2020**, *6*, n° eabb6570.

(31) Bi, X.; Feng, X.; Yang, Y.; Qiu, G.; Li, G.; Li, F.; Liu, T.; Fu, Z.; Jin, Z. Environmental Contamination of Heavy Metals from Zinc Smelting Areas in Hezhang County, Western Guizhou. *China. Environ. Inter.* **2006**, *32*, 883–890.

(32) Buhn, B.; Wall, F.; Le Bas, M. Rare-Earth Element Systematics of Carbonatitic Fluorapatites, and Their Significance for Carbonatite Magma Evolution. *Contrib. Mineral. Petrol.* **2001**, *141*, 572–591.

(33) Williams-Jones, A.; Migdisov, A.; Samson, I. Hydrothermal Mobilisation of the Rare Earth Elements - a Tale of "Ceria" and "Yttria." *Elements* **2012**, *8*, 355–360.

(34) Xiao, B.; Pan, Y.; Song, H.; Song, W.; Zhang, Y.; Chen, H. Hydrothermal Alteration Processes of Fluorapatite and Implications for REE Remobilization and Mineralization. *Contrib. Mineral. Petrol.* **2021**, *176*, n° 87.

(35) Paul, S. A. L.; Volz, J. B.; Bau, M.; Koster, M.; Kasten, S.; Koschinsky, A. Calcium Phosphate Control of REY Patterns of Siliceous-Ooze-Rich Deep-Sea Sediments from the Central Equatorial Pacific. *Geochim. Cosmochim. Acta.* **2019**, *251*, 56–72.

(36) Reynard, B.; Lecuyer, C.; Grandjean, P. Crystal-Chemical Controls on Rare-Earth Element Concentrations in Fossil Biogenic Apatites and Implications for Paleoenvironmental Reconstructions. *Chem. Geol.* **1999**, *155*, 233–241.

(37) Yasukawa, K.; Ohta, J.; Hamada, M.; Chang, Q.; Nakamura, H.; Ashida, K.; Takaya, Y.; Nakamura, K.; Iwamori, H.; Kato, Y. Essential Processes Involving REE-Enrichment in Biogenic Apatite in Deep-Sea Sediment Decoded via Multivariate Statistical Analyses. *Chem. Geol.* **2022**, *614*, n° 121184.

(38) Mackie, P. E.; Young, R. A. Location of Nd Dopant in Fluorapatite, $Ca_5(PO_4)_3F$:Nd. *J. Appl. Cryst.* **1973**, *6*, 26–31.

(39) Rønsbo, J. G. Coupled Substitution Involving REEs and Na and Si in Apatites in Alkaline Rocks from the Illimaussaq Intrusions, South Greenland, and the Petrological Implications. *Am. Miner.* **1989**, *74*, 896–901.

(40) Hughes, J. M.; Cameron, M.; Mariano, A. N. Rare-Earth-Element Ordering and Structural Variations in Natural Rare-Earth-Bearing Apatites. *Am. Miner.* **1991**, *76*, 1165–1173.

(41) Fleet, M. E.; Pan, Y. Site Preference of Nd in Fluorapatite [$Ca_{10}(PO_4)_6F_2$]. *J. Sol. State Chem.* **1994**, *112*, 78–81.

(42) Fleet, M. E.; Pan, Y. M. Site Preference of Rare-Earth Elements in Fluorapatites. *Am. Miner.* **1995**, *80*, 329–335.

(43) Fleet, M. E.; Pan. Site Preference of Rare Earth Elements in Fluorapatite: Binary (LREE+HREE)-Substituted Crystals. *Am. Miner.* **1997**, *82*, 870–877.

(44) Boyer, L.; Savariault, J. M.; Carpena, J.; Lacout, J. L. A Neodymium-Substituted Britholite Compound. *Acta Crystallogr. Sect. C* **1998**, *54*, 1057–1059.

(45) Boyer, L.; Piriou, B.; Carpena, J.; Lacout, J. L. Study of Sites Occupation and Chemical Environment of Eu^{3+} in Phosphate-Silicates Oxyapatites by Luminescence. *J. Alloys Compd.* **2000**, *311*, 143–152.

(46) Fleet, M.; Liu, X.; Pan, Y. Site Preference of Rare Earth Elements in Hydroxyapatite [$Ca_{10}(PO_4)_6(OH)_2$]. *J. Solid State Chem.* **2000**, *149*, 391–398.

(47) Bertolus, M.; Defranceschi, M. Optimizing the Formula of Rare Earth-Bearing Materials: A Computational Chemistry Investigation. *Int. J. Quantum Chem.* **2000**, *107*, 712–721.

(48) Shohel, M.; McAdams, N.; Cramer, B.; Forbes, T. Ontogenetic Variability in Crystallography and Mosaicity of Conodont Apatite: Implications for Microstructure, Palaeothermometry and Geochemistry. *R. Soc. Open Sci.* **2020**, *7*, n° 200322.

(49) Manceau, A.; Simionovici, A.; Findling, N.; Glatzel, P.; Detlefs, B.; Wegorzewski, A. V.; Mizell, K.; Hein, J. R.; Koschinsky, A. Crystal Chemistry of Thallium in Marine Ferromanganese Deposits. *ACS Earth Space Chem.* **2022**, *6*, 1269–1285.

(50) Merkulova, M.; Mathon, O.; Glatzel, P.; Batanova, V.; Marion, P.; Boiron, M. C.; Manceau, A. Revealing the Chemical Form of "Invisible" Gold in Natural Arsenian Pyrite and Arsenopyrite with High Energy-Resolution X-Ray Absorption Spectroscopy. *ACS Earth Space Chem.* **2019**, *3*, 1905–1914.

(51) Rovezzi, M.; Glatzel, P. Hard X-Ray Emission Spectroscopy: A Powerful Tool for the Characterization of Magnetic Semiconductors. *Semicond. Sci. Technol.* **2014**, *29*, 023002.

(52) Proux, O.; Lahera, E.; Del Net, W.; Kieffer, I.; Rovezzi, M.; Testemale, D.; Irar, M.; Thomas, S.; Aguilar-Tapia, A.; Bazarkina, E.; Prat, A.; Tella, M.; Auffan, M.; Rose, J.; Hazemann, J. L. High-Energy Resolution Fluorescence Detected X-Ray Absorption Spectroscopy: A Powerful New Structural Tool in Environmental Biogeochemistry Sciences. *J. Environ. Qual.* **2017**, *46*, 1146–1157.

(53) Rovezzi, M.; Lapras, C.; Manceau, A.; Glatzel, P.; Verbeni, R. High Energy-Resolution x-Ray Spectroscopy at Ultra-High Dilution with Spherically Bent Crystal Analyzers of 0.5 m Radius. *Rev. Sci. Instr.* **2017**, *88*, 013108.

(54) Holser, W. Evaluation of the Application of Rare-Earth Elements to Paleoceanography. *Palaeogeogr. Palaeoclimatol. Palaeoecol.* **1997**, *132*, 309–323.

(55) Shields, G.; Stille, P. Diagenetic Constraints on the Use of Cerium Anomalies as Palaeoseawater Redox Proxies: An Isotopic and REE Study of Cambrian Phosphorites. *Chem. Geol.* **2001**, *175*, 29–48.

(56) MacLeod, K. G.; Irving, A. J. Correlation of Cerium Anomalies with Indicators of Paleoenvironment. *J. Sediment. Res.* **1996**, *66*, 948–955.

(57) Przybylo, A.; Pietranik, A.; Zielinski, G. Cerium and Ytrium in Apatite as Records of Magmatic Processes: Insight into Fractional Crystallization, Magma Mingling and Fluid Saturation. *Geochem.* **2022**, *82*, n° 125864.

(58) Pan, Y.; Stauffer, M. R. Cerium Anomaly and Th/U Fractionation in the 1.85 Ga Flin Flon Paleosol: Clues from REE- and U-Rich Accessory Minerals and Implications for Paleoatmospheric Reconstruction. *Am. Miner.* **2000**, *85*, 898–911.

(59) Jeans, C. V.; Wray, D. S.; Williams, C. T. Redox Conditions in the Late Cretaceous Chalk Sea: The Possible Use of Cerium Anomalies as Palaeoredox Indicators in the Cenomanian and Turonian Chalk of England. *Acta Geol. Pol.* **2015**, *65*, 345–366.

(60) German, C. R.; Elderfield, H. Application of the Ce Anomaly as a Paleoredox Indicator: The Ground Rules. *Paleoceanogr.* **1990**, *5*, 823–833.

(61) Kresse, G. Ab-Initio Molecular-Dynamics for Liquid Crystals. *J. Non-Cryst. Solids* **1995**, *193*, 222–229.

(62) Kresse, G.; Furthmuller, J. Efficiency of Ab-Initio Total Energy Calculations for Metals and Semiconductors Using a Plane-Wave Basis Set. *Comput. Mater. Sci.* **1996**, *6*, 15–50.

(63) Blochl, P. E. Projector Augmented-Waves Method. *Phys. rev. B.* **1994**, *50*, 17953–17979.

(64) Kresse, G.; Joubert, D. From Ultrasoft Pseudopotentials to the Projector Augmented-Wave Method. *Phys. Rev. B.* **1999**, *59*, 1758–1775.

(65) Perdew, J. P.; Burke, K.; Ernzerhof, M. Generalized Gradient Approximation Made Simple. *Phys. Rev. Lett.* **1996**, *77*, 3865–3868.

(66) Steinmann, S. N.; Corminboeuf, C. Comprehensive Benchmarking of a Density-Dependent Dispersion Correction. *J. Chem. Theory Comput.* **2011**, *7*, 3567–3577.

(67) Gautier, S.; Steinmann, S.; Michel, C.; Fleurat-Lessard, P.; Sautet, P. Molecular Adsorption at Pt(111). How Accurate Are DFT Functionals? *Phys. Chem. Chem. Phys.* **2015**, *17*, 28921–28930.

(68) Gonthier, J. F.; Steinmann, S. N.; Wodrich, M. D.; Corminboeuf, C. Quantification of "Fuzzy" Chemical Concepts: A Computational Perspective. *Chem. Soc. Rev.* **2012**, *41*, 4671–4687.

(69) Corona-Esquivel, R.; Levresse, G.; Sole, J.; Henriquez, F.; Pi, T. New Age in the Geological Evolution of the Cerro de Mercado Iron Oxide Apatite Deposit, Mexico: Implication in the Durango Apatite Standard (DAP) Age Variability. *J. S. Am. Earth Sci.* **2018**, *88*, 367–373.

(70) Ouabid, M.; Raji, O.; Dautria, J.; Bodinier, J.; Parat, F.; El Messbahi, H.; Garrido, C.; Ahechach, Y. Petrological and Geochemical Constraints on the Origin of Apatite Ores from Mesozoic Alkaline Intrusive Complexes, Central High-Atlas, Morocco. *Ore Geol. Rev.* **2021**, *136*.

(71) El Bamiki, R.; Raji, O.; Ouabid, M.; Elghali, A.; Yazami, O.; Bodinier, J. Phosphate Rocks: A Review of Sedimentary and Igneous Occurrences in Morocco. *Minerals* **2021**, *11*, n° 1137.

(72) Tyszka-Czochara, M.; Suder, M.; Dolhanczuk-Srodka, A.; Rajfur, M.; Grata, K.; Starosta, M.; Jagoda-Pasternak, A.; Kasprzyk, W.; Nowak, A.; Ahmadzadeh, S.; Kopec, D.; Surylo, P.; Swiergosz, T.; Stadnicka, K. Nature-Inspired Effects of Naturally Occurring Trace Element-Doped Hydroxyapatite Combined with Surface Interactions of Mineral-Apatite Single Crystals on Human Fibroblast Behavior. *Int. J. Mol. Sci.* **2022**, *23*, n° 802.

(73) Glatzel, P.; de Groot, F. M. F.; Manoilova, O.; Grandjean, D.; Weckhuysen, B. M. Range-Extended EXAFS at the L Edge of Rare Earths Using High-Energy-Resolution Fluorescence Detection: A Study of La in LaOCl. *Phys. Rev. B* **2005**, *72*, n° 014117.

(74) Shannon, R. D. Revised Effective Ionic Radius and Systematic Studies of Interatomic Distances in Halides and Chalcogenides. *Acta Crystallogr.* **1976**, *B25*, 925–946.

(75) Manceau, A.; Combes, J. M. Structure of Mn and Fe Oxides and Oxyhydroxides: A Topological Approach by EXAFS. *Phys. Chem. Miner.* **1988**, *15*, 283–295.

(76) Manceau, A.; Lanson, B.; Drits, V. A. Structure of Heavy Metal Sorbed Birnessite. Part III. Results from Powder and Polarized Extended X-Ray Absorption Fine Structure Spectroscopy. *Geochim. Cosmochim. Acta.* **2002**, *66*, 2639–2663.

(77) Ankudinov, A. L.; Rehr, J. J. Relativistic Calculations of Spin-Dependent X-Ray-Absorption Spectra. *Phys. Rev. B* **1997**, *56*, 1712–1716.

(78) Putnis, C.; Putnis, A. A Mechanism of Ion Exchange by Interface-Coupled Dissolution-Precipitation in the Presence of an Aqueous Fluid. *J. Cryst. Growth* **2022**, *600*.

(79) Tamm, T.; Peld, M. Computational Study of Cation Substitutions in Apatites. *J. Sol. State Chem.* **2006**, *179*, 1581–1587.

(80) Takaya, Y.; Yasukawa, K.; Kawasaki, T.; Fujinaga, K.; Ohta, J.; Usui, Y.; Nakamura, K.; Kimura, J. I.; Chang, Q.; Hamada, M.; Dodbiba, G.; Nozaki, T.; Iijima, K.; Morisawa, T.; Kuwahara, T.; Ishida, Y.; Ichimura, T.; Kitazume, M.; Fujita, T.; Kato, Y. The Tremendous Potential of Deep-Sea Mud as a Source of Rare-Earth Elements. *Sci. Rep.* **2018**, *8*, n° 5763.

(81) Schoonjans, T.; Brunetti, A.; Golosio, B.; del Rio, M.; Sole, V.; Ferrero, C.; Vincze, L. The Xraylib Library for X-Ray-Matter Interactions. Recent Developments. *Spectrochim. Acta B: At. Spectrosc.* **2011**, *66*, 776–784.

(82) Brunetti, A.; Sanchez del Rio, M.; Golosio, B.; Simionovici, A.; Somogyi, A. A Library for X-Ray-Matter Interaction Cross Sections for X-Ray Fluorescence Applications. *Spectrochim. Acta B* **2007**, *59*, 1725–1731.

Table 1. Total Energies of the Ce-Si and Ce-Na Models

Model	**Total energy *E*(eV/cell)**	**Energy difference**
Na prefers the Ca1 site, regardless of the Ce site		
Ce2-Na1-close	-2447.40	-0.18
Ce2-Na2-close	-2447.22	-
Ce1-Na1-close	-2447.40	-0.30

Ce1-Na2-close	-2447.10	-
Ce has no site preference in the Ce-Na model		
Ce2-Na1-close	-2447.40	0.00
Ce1-Na1-close	-2447.40	
Ce prefers the Ca2 site in the Ce-Si model		
Ce2-Si-close	-2451.30	-0.08
Ce1-Si-close	-2451.22	
Ce2-Na1 charge compensation at short distance		
Ce2-Na1-close	-2447.40	-0.09
Ce2-Na1-far	-2447.31	-
Ce1-Na1 charge compensation at short distance		
Ce1-Na1-close	-2447.40	-0.18
Ce1-Na1-far	-2447.22	-
Ce2-Si charge compensation at short distance		
Ce2-Si-close	-2451.30	-0.36
Ce2-Si-far	-2450.94	
Ce1-Si charge compensation at short distance		
Ce1-Si-close	-2451.22	-0.34
Ce1-Si-far	-2450.88	-

FIGURE CAPTION

Figure 1. (a) Structure of FAp projected in the *ab* plane.[19] (b) CaO_6-PO_4 and CaO_6F-PO_4 linkages at the Ca1 and Ca2 sites of FAp, and CeO_7-(PO_4,SiO_4) linkage of the Ce1-Si-close model. The F atom is located in the middle of the tunnel (a) and is unshared (b).

Figure 2. (a) Monte Carlo simulation of the XRF spectrum for the Durango FAp calculated with the resolution of a SDD and an excitation energy of 6 keV using the Xraylib database.[81,82] (b) Ce L_3-edge X-ray absorption spectrum of the Durango FAp measured with a SDD and a five-crystal spectrometer (HERFD-XAS).[53]

Figure 3. Polyedral sketch of the DFT local structure of Ce in the Ca1 and Ca2 sites (a), and population histogram of the Ce-(O,F,Si,P,Ca) distances (b,c). (a) Brown, Ca in the Ca1 site; green,

Ca in the Ca2 site; cyan, Ce in the Ca1/Ca2 site; purple, P corner-linked to Ca2/Ce2; blue, Si edge-linked to Ce2/Ce1; red, oxygen; light green, F. (b) Ce-2-Si-close DFT model. Average distance of the 6 nearest O,F = 2.428 Å, σ = 0.035 Å. (c) Ce1-Si-close DFT model. Average distance of the 9 O = 2.549 Å, σ = 0.078 Å. Number of atoms on the histograms are counted in intervals of 0.05 Å.

Figure 4. Dependence of the relative stability of substituents in the Ca1 and Ca2 site of FAp on their electronic properties. (a) Effect of the effective ionic radius expressed as the difference between the Me(II) and Ca(II) radii (ΔIR). (b) Effect of the atomic charge expressed as the difference of its value for Me(II) in the Ca2 and Ca1 sites (ΔAC). (c,d) Effect of the first (c) and second (d) ionization energies expressed as the difference between the Me(II) and Ca(II) energies (ΔIE).

Figure 5. Experimental Ce L_3-edge EXAFS spectra and Fourier transforms (magnitude and imaginary parts) of the Durango FAp measured at room temperature (Durango-RT) and at 8-12 K (Durango-HeT) (a,b), and of Durango-RT and the Imilchil FAp measured at room temperature (Imilchil-RT) (c,d).

Figure 6. Experimental and DFT-derived theoretical Ce L_3-edge EXAFS spectra and Fourier transforms (magnitude and imaginary parts) of FAp. (a,b) Durango FAp measured at room temperature (Durango-RT) and Ce2-Si-close spectra. (c,d) Durango-RT and Ce1-Si-close spectra.

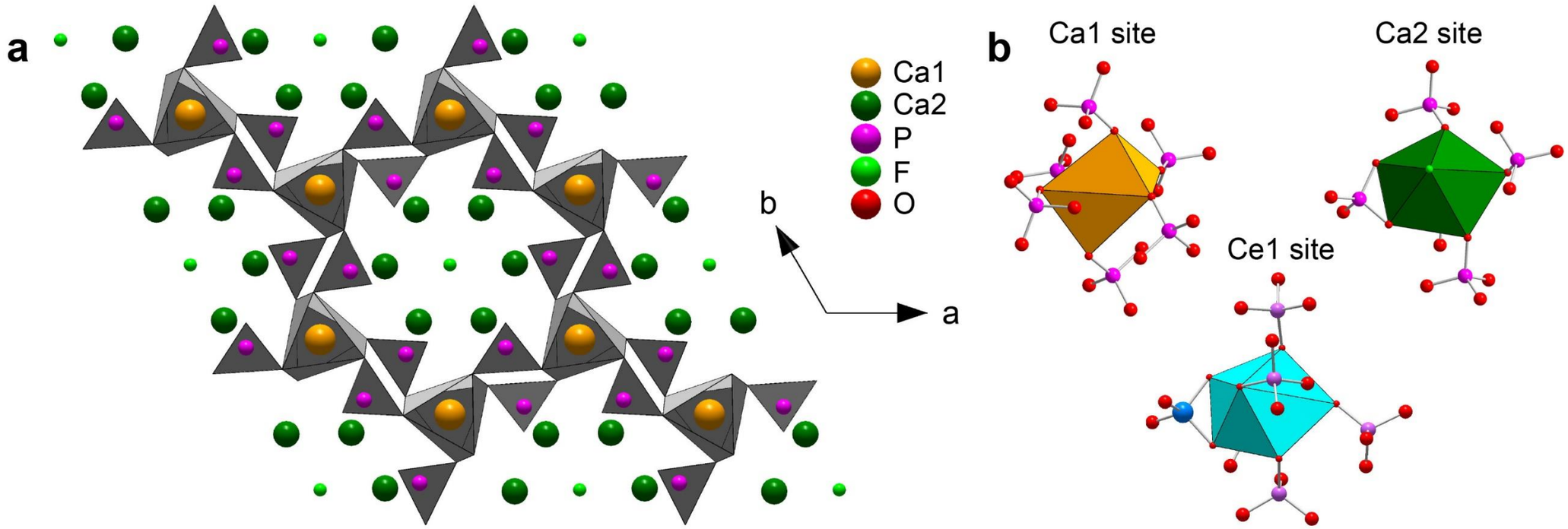

Figure 1

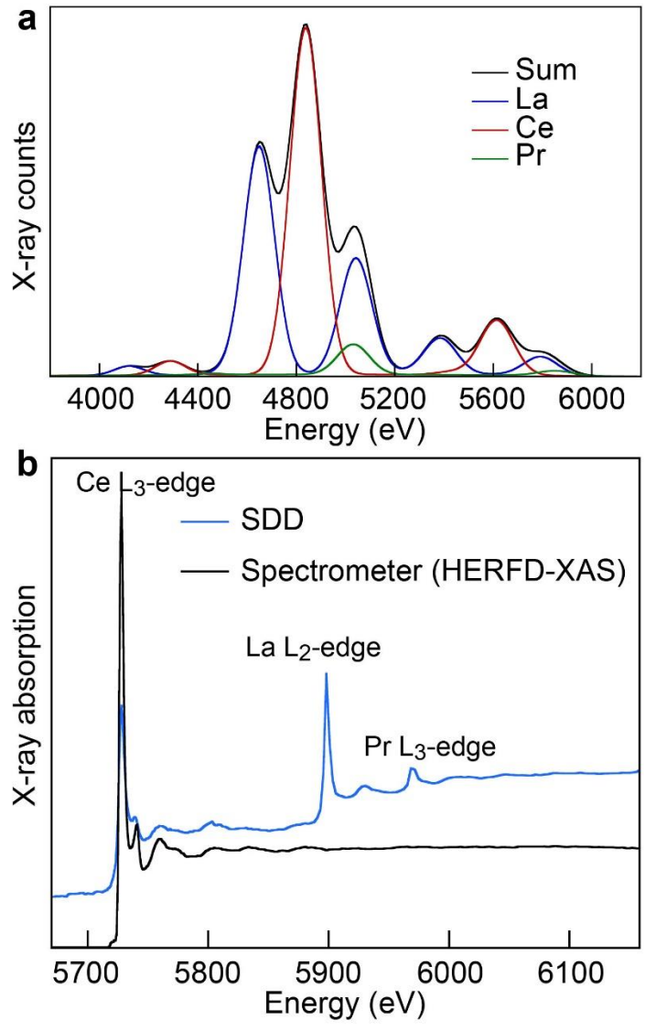
a
X-ray counts
Sum
La
Ce
Pr
4000
4400
4800
5200
5600
6000
Energy (eV)
b
X-ray absorption
Ce L3-edge
SDD
Spectrometer (HERFD-XAS)
La L2-edge
Pr L3-edge
5700
5800
5900
6000
6100
Energy (eV)

Figure 2

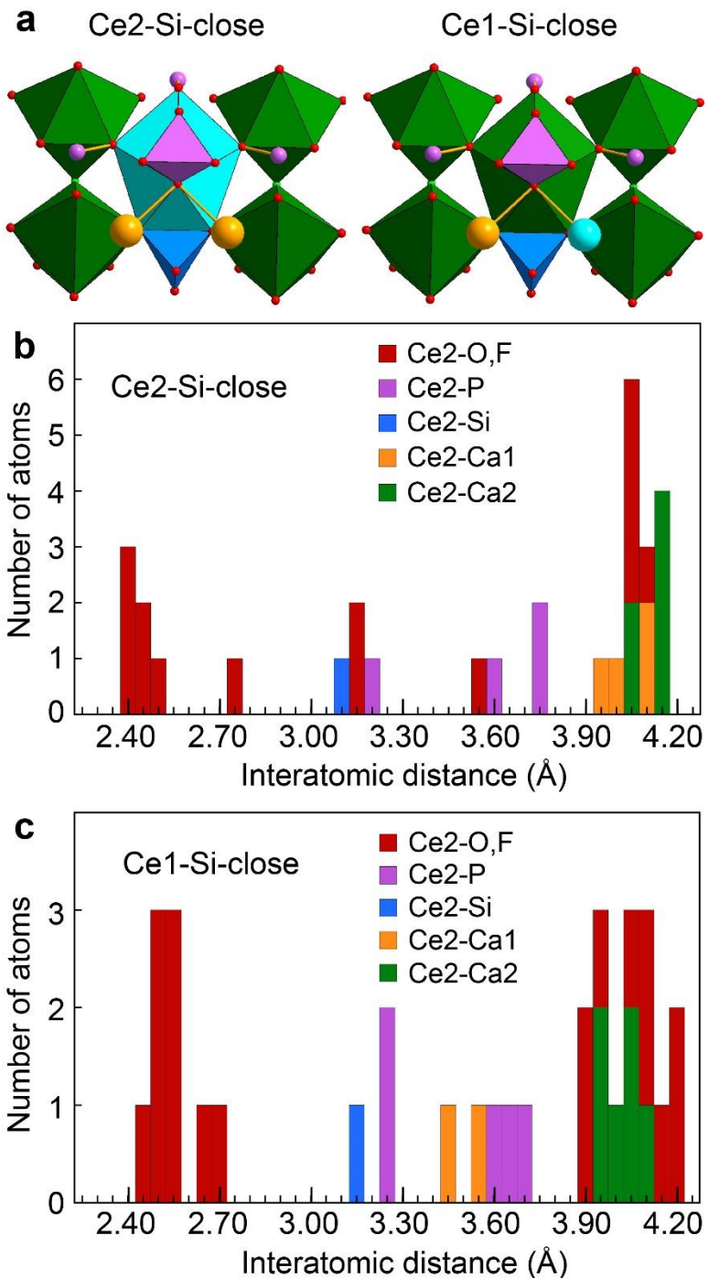
a
Ce2-Si-close
Ce1-Si-close
b
Ce2-Si-close
Ce2-O,F
Ce2-P
Ce2-Si
Ce2-Ca1
Ce2-Ca2
Number of atoms
0
1
2
3
4
5
6
2.40
2.70
3.00
3.30
3.60
3.90
4.20
Interatomic distance (Å)
c
Ce1-Si-close
Ce2-O,F
Ce2-P
Ce2-Si
Ce2-Ca1
Ce2-Ca2
Number of atoms
0
1
2
3
2.40
2.70
3.00
3.30
3.60
3.90
4.20
Interatomic distance (Å)

Figure 3

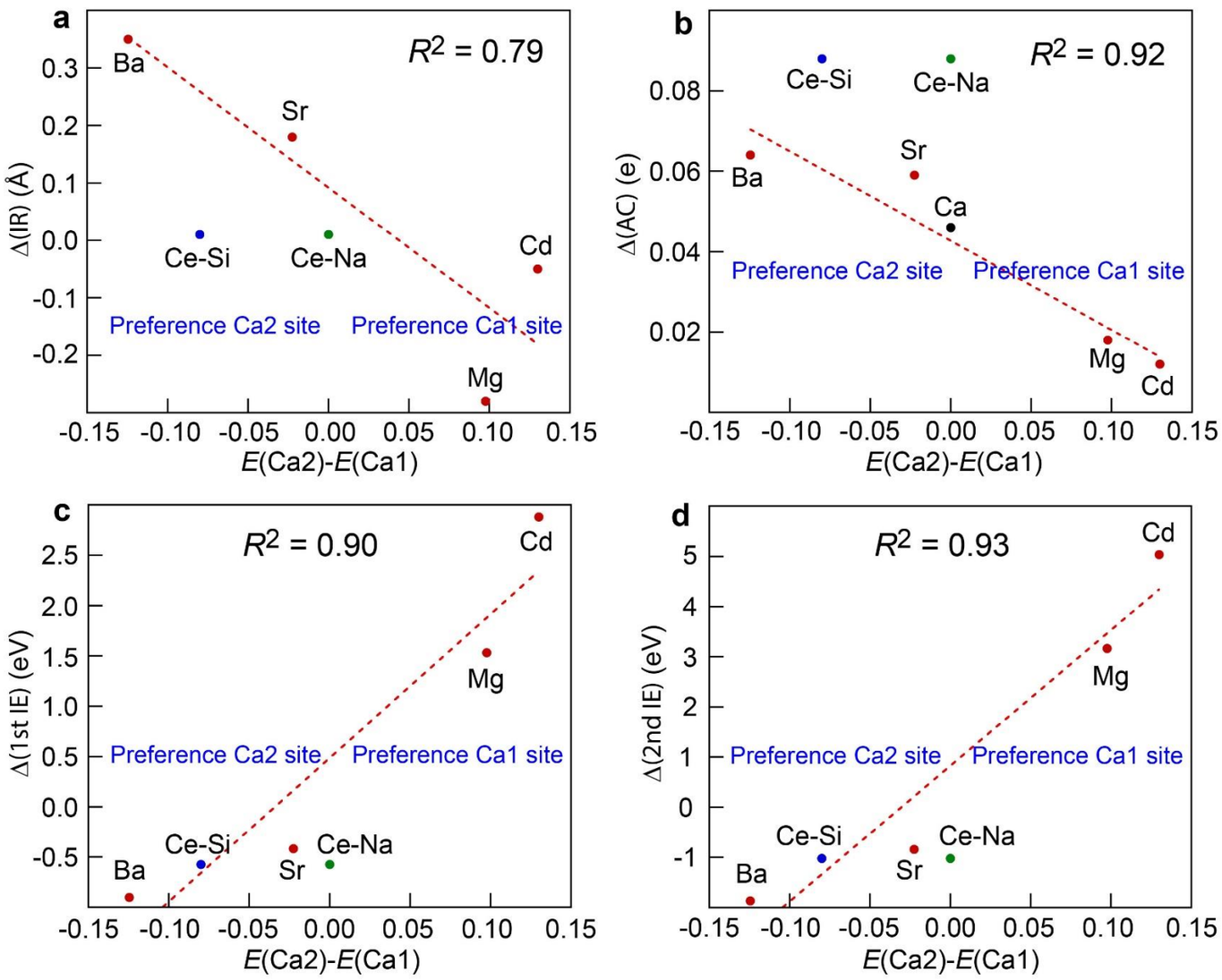
a
R^2 = 0.79
Δ(IR) (Å)
Ba
Sr
Ce-Si
Ce-Na
Cd
Mg
Preference Ca2 site
Preference Ca1 site
E(Ca2)-E(Ca1)
b
R^2 = 0.92
Δ(AC) (e)
Ce-Si
Ce-Na
Ba
Sr
Ca
Preference Ca2 site
Preference Ca1 site
Mg
Cd
E(Ca2)-E(Ca1)
c
R^2 = 0.90
Δ(1st IE) (eV)
Cd
Mg
Preference Ca2 site
Preference Ca1 site
Ce-Si
Ce-Na
Ba
Sr
E(Ca2)-E(Ca1)
d
R^2 = 0.93
Δ(2nd IE) (eV)
Cd
Mg
Preference Ca2 site
Preference Ca1 site
Ce-Si
Ce-Na
Ba
Sr
E(Ca2)-E(Ca1)

Figure 4

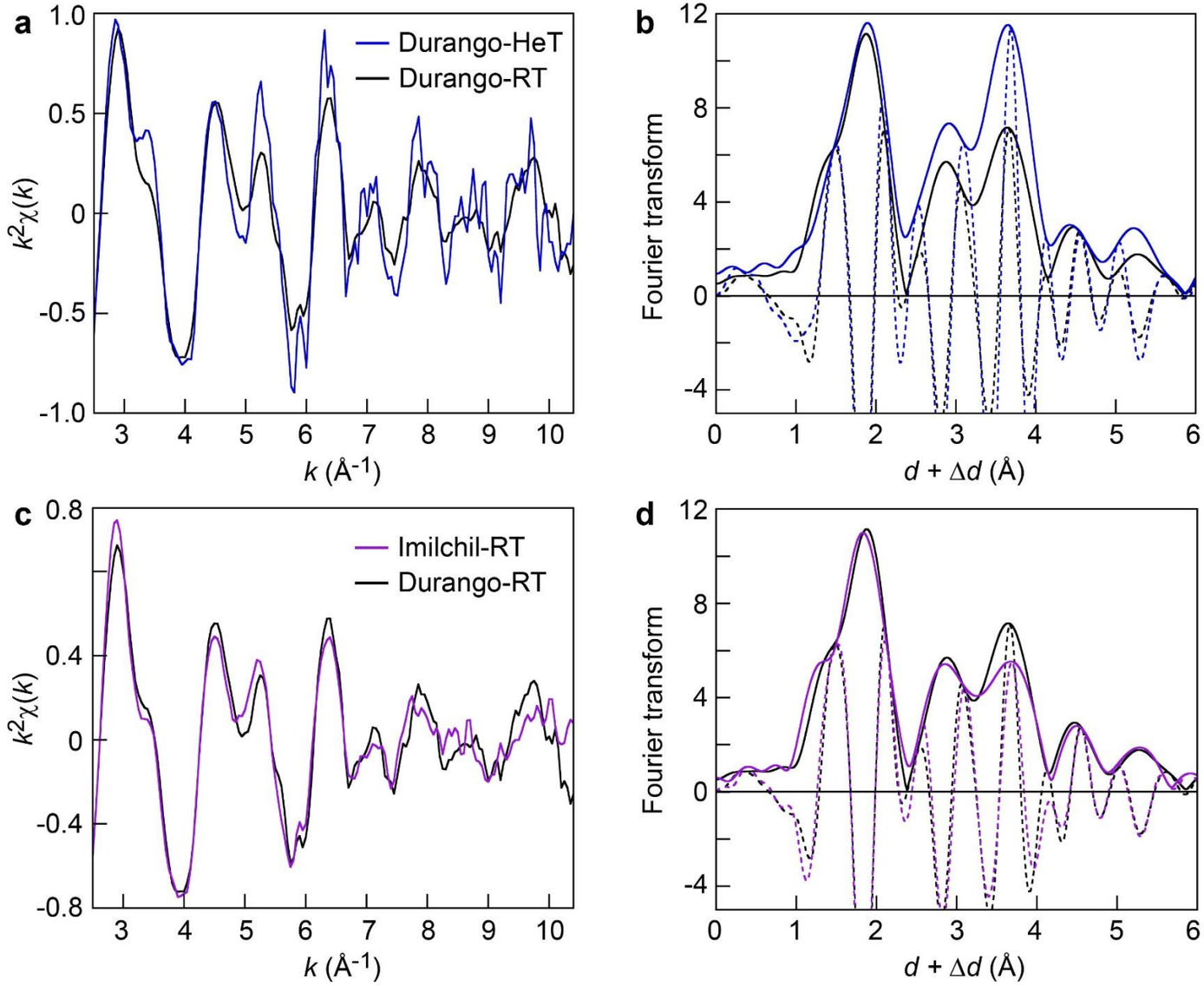
a
Durango-HeT
Durango-RT
$k^2\chi(k)$
k (Å^{-1})
b
Fourier transform
$d + \Delta d$ (Å)
c
Imilchil-RT
Durango-RT
$k^2\chi(k)$
k (Å^{-1})
d
Fourier transform
$d + \Delta d$ (Å)

Figure 5

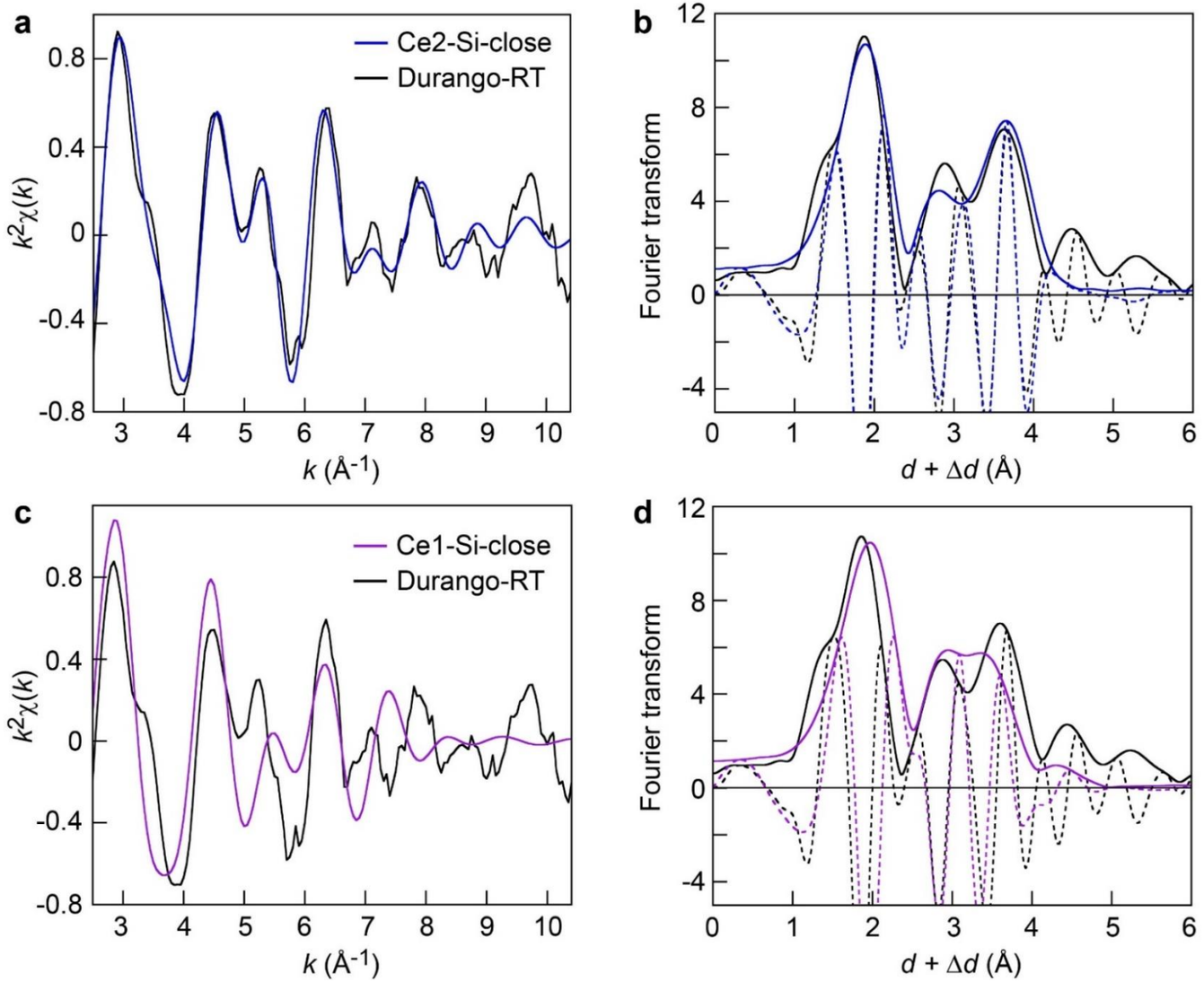
a
Ce2-Si-close
Durango-RT
$k^2\chi(k)$
k (Å^{-1})
b
Fourier transform
$d + \Delta d$ (Å)
c
Ce1-Si-close
Durango-RT
$k^2\chi(k)$
k (Å^{-1})
d
Fourier transform
$d + \Delta d$ (Å)

Figure 6

Supporting Information

Revealing the incorporation of cerium in fluorapatite

Alain Manceau*[1,2], Olivier Mathon[1], Kirill A. Lomachenko[1], Mauro Rovezzi[3], Kristina O. Kvashnina[4,5], Marie-Christine Boiron[6], Romain Brossier[7], and Stephan N. Steinmann*[2]

[1]European Synchrotron Radiation Facility (ESRF), 38000 Grenoble, France
[2]ENS de Lyon, CNRS, Laboratoire de Chimie, 69342 Lyon, France
[3]Université Grenoble Alpes, CNRS, OSUG, FAME, 38000 Grenoble, France
[4]The Rossendorf Beamline, ESRF, 38000 Grenoble, France
[5]Helmholtz Zentrum Dresden-Rossendorf (HZDR), Institute of Resource Ecology, 01314 Dresden, Germany
[6]Univ. Lorraine, ENSG, CNRS, GeoRessources Lab, 54000 Nancy, France
[7]Université Grenoble Alpes, CNRS, ISTerre, 38000 Grenoble, France

EXAFS Spectroscopy

Measurement of the Durango FAp at RT on ID24-DCM. The incident photon energy was selected using the Si(111) reflection from a liquid-nitrogen-cooled double-crystal monochromator, and the rejection of higher harmonics was achieved with two Si mirrors at an incidence angle of 4 mrad (7 keV cutoff). The beam size on the sample was 80 (H) × 80 (V) μm^2, and the incident X-ray flux was $\sim 5 \times 10^{12}$ photons per s at the sample position. The Ce $L_{\alpha 1}$ ($3d_{5/2} \rightarrow 2p_{3/2}$) fluorescence line (4839 eV) was selected using the 400 reflection of five Si crystals of 100 mm diameter, spherically bent to a radius of 0.5 m and aligned at a Bragg angle of 70.6° in a vertical Rowland geometry.[1] The diffracted intensity was measured with a Si drift diode detector (SDD) in single photon counting mode. Forty-four spectra of 7 min were acquired in continuous scan mode, and averaged to improve statistics.

Measurement of the Durango FAp at 8-12 K on FAME-UHD (BM16). The incident photon energy was selected using the Si(220) reflection from a liquid-nitrogen-cooled double-crystal monochromator, and the rejection of higher harmonics was achieved with two Rh-coated cylindrical mirrors at an incidence angle of 6.2 mrad (9.5 keV cutoff). The beam size on the sample was 300 (H) × 100 (V) μm^2, and the incident X-ray flux was $\sim 10^{11}$ photons per s at the sample position. The Ce $L_{\alpha 1}$ fluorescence line was selected using the 331 reflection of five Ge crystals of 100 mm diameter, spherically bent to a radius of 1.0 m and aligned at a Bragg angle of 80.7° in a vertical Rowland geometry.[2] The diffracted intensity was measured with a Si drift diode detector (SDD) in single photon counting mode. Forty-seven spectra of 31 min were acquired and averaged to improve statistics. Measurements were performed using a helium flow cryostat.

Measurement of the Imilchil FAp on BM20. The incident photon energy was selected using the Si(111) reflection from a liquid-nitrogen-cooled double-crystal monochromator, and the rejection of higher harmonics was achieved by two Si mirrors at an incidence angle of 2.5 mrad. The beam size on the sample was 400 (H) × 150 (V) μm^2, and the incident X-ray flux was $\sim 10^{10}$ photons per s at the sample position. The Ce $L_{\alpha 1}$ fluorescence line was selected using the 331 reflection of five Ge crystals of 100 mm diameter, spherically bent to a radius of 0.5 m and aligned at a Bragg angle of 80.7° in a vertical Rowland geometry.[1,3] Eigthy-three spectra of 20 min were acquired and averaged to improve statistics.

EXAFS spectra collected on different beamlines were intercalibrated on the same energy scale. Data were reduced with the Athena software.[4]

LA-ICP-MS analysis

Laser sampling was performed with a 193 nm GeoLas Pro ArF Excimer laser (Microlas®, Göttingen, Germany) equipped with beam homogenization optics. An ablation crater of 60 μm was performed by focusing the beam on the sample surface with a constant fluence of 10 mJ/cm^2 and constant repetition rate of 5 Hz. Helium was used as a carrier gas to transport the laser-generated aerosols from the ablation cell to the ICP-MS analyzer. Argon as make-up gas was mixed with the carrier gas before entering the ICP torch. A typical flow rate of 0.5 $l.min^{-1}$ for He and 0.96 $l.min^{-1}$ for Ar was used. These values were optimized with the analysis of NIST610 SRM silicate glass. Ablated material was analyzed by an Agilent 7500c Quadrupole ICP-MS (Agilent®, Santa Clara, California) equipped with an Octopole Reaction

System with enhanced sensitivity optional lenses (Cs type, Agilent). Peak hopping ablation mode began 20 s after the beginning of the signal acquisition, in order to sample the background signal before ablation (used for data reduction), and was stopped after 200 pulses (40 s). External standard calibration was performed with the NIST610 SRM reference. Data reduction was carried out using Iolite software (version 4),[5] following the standard methods of Longerich et al., (1996).[6]

Supplementary References

(1) Rovezzi, M.; Lapras, C.; Manceau, A.; Glatzel, P.; Verbeni, R. High Energy-Resolution x-Ray Spectroscopy at Ultra-High Dilution with Spherically Bent Crystal Analyzers of 0.5 m Radius. *Rev. Sci. Instr.* **2017**, *88*, 013108.

(2) Proux, O.; Lahera, E.; Del Net, W.; Kieffer, I.; Rovezzi, M.; Testemale, D.; Irar, M.; Thomas, S.; Aguilar-Tapia, A.; Bazarkina, E.; Prat, A.; Tella, M.; Auffan, M.; Rose, J.; Hazemann, J. L. High-Energy Resolution Fluorescence Detected X-Ray Absorption Spectroscopy: A Powerful New Structural Tool in Environmental Biogeochemistry Sciences. *J. Environ. Qual.* **2017**, *46*, 1146–1157.

(3) Kvashnina, K.; Scheinost, A. A Johann-Type X-Ray Emission Spectrometer at the Rossendorf Beamline. *J. Synchrotron Rad.* **2016**, *23*, 836–841.

(4) Ravel, B.; Newville, M. ATHENA, ARTEMIS, HEPHAESTUS: Data Analysis for X-Ray Absorption Spectroscopy Using IFEFFIT. *J. Synchrotron Radiat.* **2005**, *12*, 537–541.

(5) Paton, C.; Hellstrom, J.; Paul, B.; Woodhead, J.; Hergt, J. Iolite: Freeware for the Visualisation and Processing of Mass Spectrometric Data. *J. Anal. At. Spectrom.* **2011**, *26*, 2508–2518.

(6) Longerich; Jackson, S. E.; Gunther, D. Laser Ablation Inductively Coupled Plasma Mass Spectrometric Transient Signal Data Acquisition and Analyte Concentration Calculation. *J. Anal. At. Spectrom.* **1996**, *11*, 899–904.

Table S1. Optimized (VASP) versus experimental (XRD)[a] interatomic distances (Å) for FAp

Ca1 site	**VASP**	**XRD**	**%Diff**
3O1	2.397	2.399	0.08
3O2	2.446	2.457	0.45
3O3	2.806	2.807	0.04
3P	3.206	3.207	0.03
Ca1	3.427	3.425	-0.06
Ca1	3.447	3.453	0.17
3P	3.586	3.585	-0.03
3O3	3.931	3.916	-0.38
Ca2 site			
F	2.305	2.311	0.26
2O3	2.341	2.348	0.30
O2	2.372	2.374	0.08
2O3	2.493	2.501	0.32
O1	2.731	2.700	-1.15
P	3.053	3.075	0.72
P	3.285	3.265	-0.61
2O3	3.33	3.347	0.51
O1	3.493	3.493	0.00
P	3.5	3.494	-0.17
2P	3.684	3.68	-0.11
2Ca1	3.974	3.961	-0.33

[a]Hughes et al. *Am. Miner*., 1989, 74, 870-876.

Table S2. Chemical analysis of the Imilchil FAp in mg/kg (ppm).

Technique	**Element**	**Point 1**	**Point 2**	**Point 3**	**Point 4**	**Average**	**STD**
ICP-AES	Na	1332	1353	1076	1531	1323	187
ICP-AES	Mg	92	93	70	88	85.8	10.9
ICP-AES	K	10	2	8	4	6.0	3.6

ICP-AES	Sc	0.2	0.2	0.3	0.3	0.3	0.1
ICP-AES	Ti	18	24	22	23	22	3
ICP-AES	V	3	3	3	4	3.3	0.4
ICP-AES	Fe	613	628	606	694	635	40
ICP-AES	Co	0.2	0.1	0.2	0.1	0.2	0.1
ICP-AES	Ni	0.5	3.2	3.4	0.2	1.8	1.7
ICP-AES	Cu	0.4	0.1	0.1	0.0	0.2	0.2
ICP-AES	Zn	0.1	0.0	0.1	0.2	0.1	0.1
ICP-AES	As	12	12	11	14	12.4	1.3
ICP-AES	Sn	4	4	5	6	4.8	0.6
ICP-AES	Ba	0.8	0.9	0.9	1.4	1.0	0.3
LA-ICP-MS	Mn	220	211	234	233	225	11
LA-ICP-MS	Sr	672	668	664	668	668	3
LA-ICP-MS	Y	1226	1280	1219	1289	1254	36
LA-ICP-MS	La	2307	2366	3006	3033	2678	395
LA-ICP-MS	Ce	4764	4617	5068	5006	4864	210
LA-ICP-MS	Pr	487	491	500	490	492	5
LA-ICP-MS	Nd	1917	1964	1898	1917	1924	28
LA-ICP-MS	Sm	397	409	382	389	395	12
LA-ICP-MS	Eu	41	41	38	39	40.0	1.5
LA-ICP-MS	Gd	389	401	370	380	385	13
LA-ICP-MS	Tb	49	50	47	48	48.3	1.2
LA-ICP-MS	Dy	264	274	259	269	266	7
LA-ICP-MS	Ho	47	49	47	49	47.8	1.0
LA-ICP-MS	Er	108	113	110	114	111	3
LA-ICP-MS	Tm	12	12	12	13	12.2	0.3
LA-ICP-MS	Yb	57	59	61	62	59.7	2.2
LA-ICP-MS	Lu	5	6	6	6	5.7	0.4
LA-ICP-MS	Th	59	61	82	88	72.7	14.5
LA-ICP-MS	U	7	7	9	9	7.8	1.0

Table S3. Total energies and atomic charges of the Me(II)-FAp models

Model	Total energy E (eV/cell)	Energy difference	Atomic charge AC (e-)	AC difference
Mg2	-2444.91	0.10	0.64	0.02
Mg1	-2445.01	-	0.62	-
Cd2	-2441.03	0.13	0.82	0.01
Cd1	-2441.16	-	0.81	-
Sr2	-2446.67	-0.02	0.49	0.06
Sr1	-2446.65	-	0.43	-
Ba2	-2446.75	-0.12	0.44	0.06
Ba1	-2446.63	-	0.38	-

Table S4. Atomic charges of the Ce-Si and Ce-Na models

Model	Atomic charge AC (e-)	AC difference
Ce2-Si-close	0.77	0.08
Ce1-Si-close	0.69	-
Ce2-Na1-close	0.78	0.09
Ce1-Na1-close	0.69	-

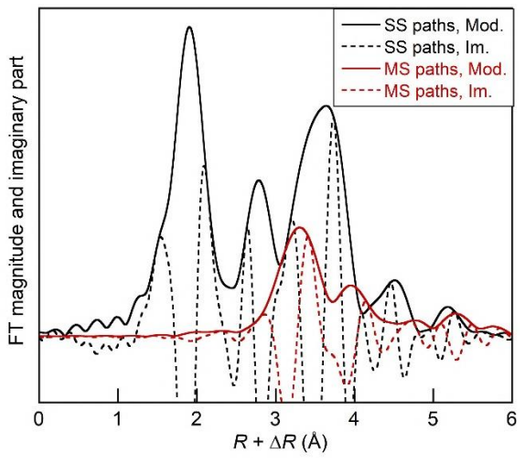

Fig. S1. Fourier transforms (modulus and imaginary parts) of the EXAFS single (SS) and multiple (MS) scattering paths calculated with FEFF 8.2.

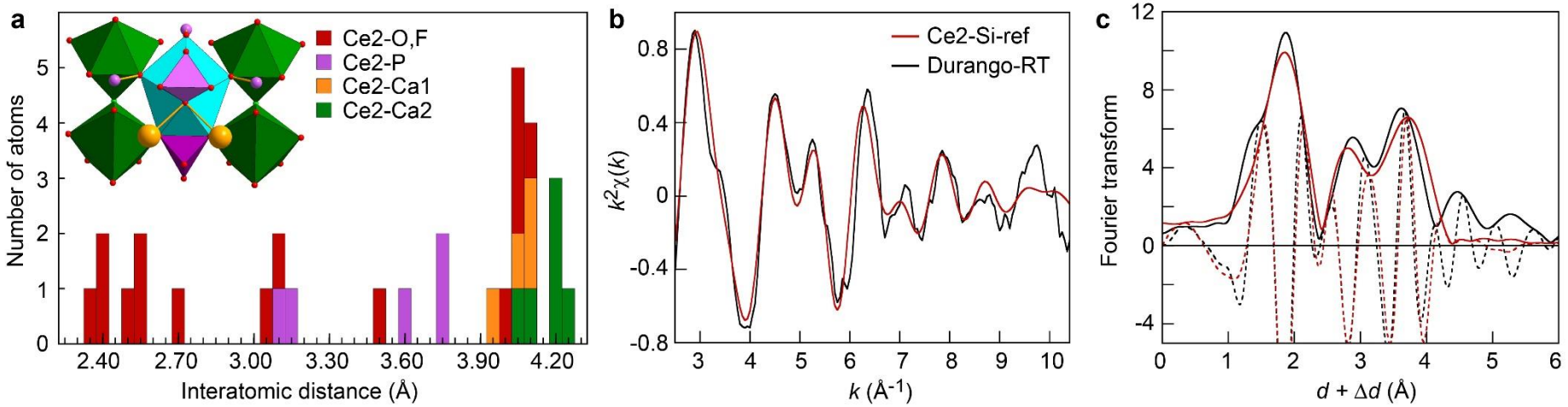

Fig. S2. (a) Population histogram of the Ce-(O,F,P,Ca) distances for the Ce2-Si-ref model and polyedral sketch of the local structure of Ce in the Ca2 site. Brown, Ca in the Ca1 site; green, Ca2 polyhedron; cyan, Ce2 polyhedron; dark purple, P tetrahedron edge-linked to Ce2 polyhedron and corner-linked to Ca1, light purple, P tetrahedron corner-linked to Ce2 polyhedron; red, oxygen; light green, F. (b,c) EXAFS spectra and Fourier transforms (magnitude and imaginary parts) of Durango-RT and the Ce2-Si-ref model.

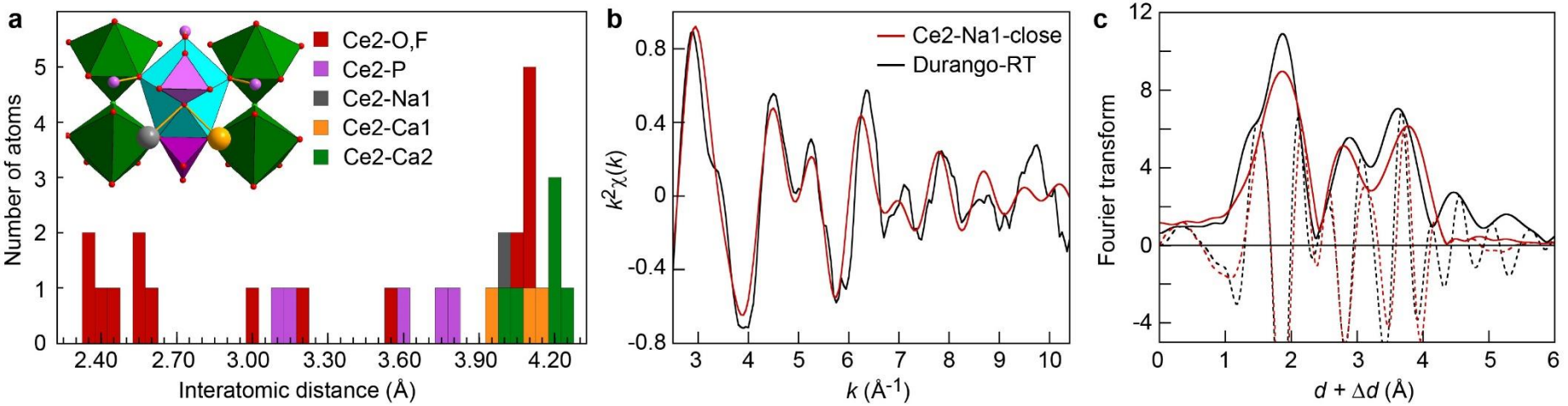

Fig. S3. (a) Population histogram of the Ce-(O,F,P, Na, Ca) distances for the Ce2-Na1-close model and polyedral sketch of the local structure of Ce in the Ca2 site with Na at short distance. Brown, Ca in the Ca1 site; green, Ca2 polyhedron; cyan, Ce2 polyhedron; grey, Na in the Ca1 site

(Na1); dark purple, P tetrahedron edge-linked to Ce2 polyhedron and corner-linked to Ca1 and Na1, light purple, P tetrahedron corner-linked to Ce2 polyhedron; red, oxygen; light green, F (b,c) EXAFS spectra and Fourier transforms (magnitude and imaginary parts) of Durango-RT and the Ce2-Na1-close model.

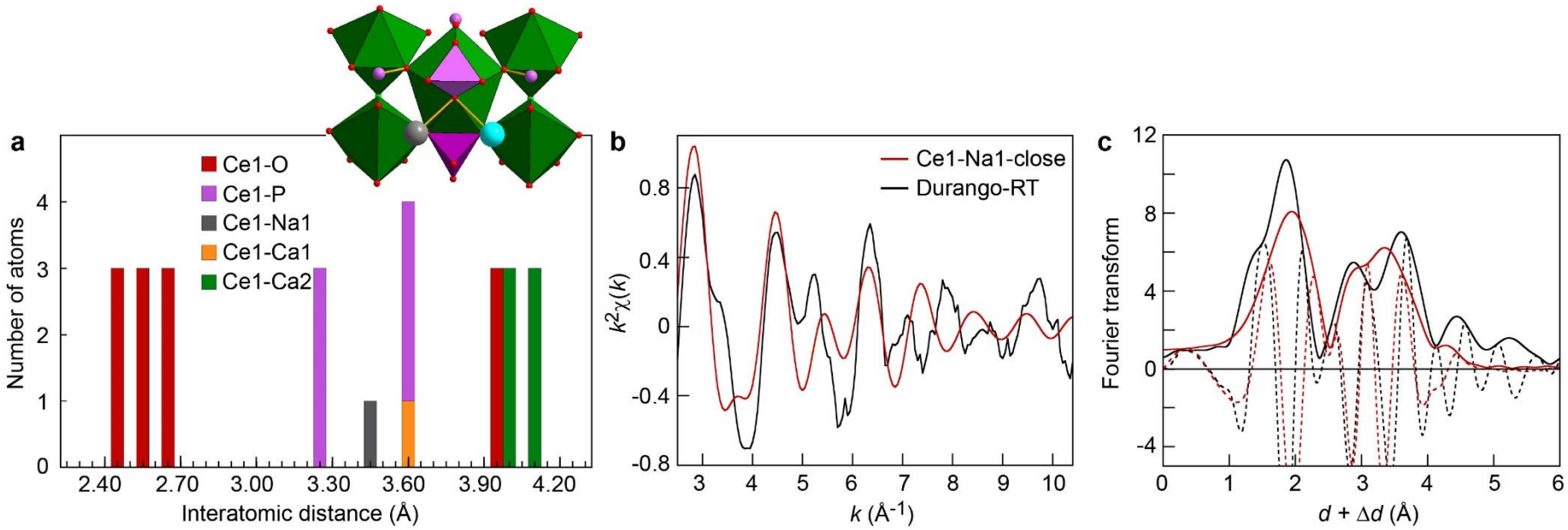

Fig. S4. (a) Population histogram of the Ce-(O,F,P, Na, Ca) distances for the Ce1-Na1-close model and polyedral sketch of the local structure of Ce in the Ca1 site with Na at short distance. Green, Ca2 polyhedron; cyan, Ce in the Ca1 site (Ce1); grey: Na in the Ca1 site (Na1); dark purple, P tetrahedron edge-linked to Ca2 polyhedron and corner-linked to Ce1 and Na1, light purple, P tetrahedron corner-linked to Ca2 polyhedron; red, oxygen; light green, F (b,c) EXAFS spectra and Fourier transforms (magnitude and imaginary parts) of Durango-RT and the Ce1-Na1-close model.

Cartesian coordinates (*a* = 100 Å, *b* = 100 Å, *c* = 100 Å) - Ce1-Na1-close model

58	9.392709952	5.422883296	6.839256000
11	9.392709952	5.422883296	3.379071143
20	5.877256564	6.156736541	5.096284453
20	4.704226934	2.701219347	-0.004956409
20	4.697584079	2.696475410	6.862156680
20	14.093982154	2.723370343	-0.004956409
20	14.101411952	2.719989430	6.862156680
20	0.000000149	10.845767321	13.759103192
20	0.000000149	10.845767321	6.871653625
20	9.379921219	10.844061401	-0.004956409
20	9.379134277	10.852186251	6.862156680
20	-0.006831995	5.424821060	6.853543179
20	0.003369815	5.419532776	13.733762578
20	9.392709952	5.422883296	0.076788019
20	-4.691260832	13.562156529	6.853543179
20	-4.700941526	13.555965644	13.733762578
20	4.698092822	13.550323170	6.853543179
20	4.697571705	13.561802339	13.733762578
20	8.222441124	1.994306495	1.709854358
20	8.182734047	1.935578419	8.605319945
20	17.599224232	1.972908709	1.701696449
20	17.603587025	1.969186298	8.584268320
20	3.511620251	10.120966507	1.700871240
20	3.507541904	10.104939874	8.582015432
20	12.895781687	10.078816032	1.707031633
20	12.915528214	10.129204287	8.589157044
20	3.609018414	6.128666644	1.707031633
20	3.555507641	6.120573510	8.589157044
20	12.947079332	6.123689764	1.709854358
20	13.017792876	6.118666465	8.605319945
20	-1.128114201	14.249320075	1.700871240
20	-1.112195556	14.253801439	8.582015432
20	8.277218804	14.254921035	1.701696449
20	8.278261110	14.260560529	8.584268320
20	1.116856954	2.012424048	5.141618383
20	1.114802960	2.011682999	12.029491596
20	10.514901521	2.011485213	5.096284453
20	10.514586651	1.999167569	12.036604549
20	-3.579384290	10.144382680	5.145426921
20	-3.576829331	10.148416499	12.031569390
20	5.801232736	10.161026673	5.136950696
20	5.811620560	10.151903220	12.037500494
20	2.301686764	0.040821234	1.701696449
20	2.296281665	0.038904151	8.584268320
20	11.673329699	0.061168302	1.707031633
20	11.707093944	0.018873181	8.589157044
20	-2.383506111	8.167015267	1.700871240
20	-2.395346409	8.178560536	8.582015432
20	7.008609344	8.150654719	1.709854358
20	6.977602877	8.214406094	8.605319945
20	2.397109069	8.096621674	5.145426921
20	2.392338199	8.096817423	12.031569390
20	11.785971926	8.100429102	5.096284453
20	11.796796754	8.106315238	12.036604549
20	-2.307613566	16.212152325	5.136950696
20	-2.304906335	16.225710171	12.037500494
20	7.091471205	16.229665209	5.141618383
20	7.093139969	16.228256922	12.029491596
20	-3.493619021	6.164122728	5.136950696
20	-3.506714076	6.159688336	12.037500494
20	5.866746606	6.163168048	12.036604549
20	-8.208328009	14.295212470	5.141618383
20	-8.207942778	14.297361805	12.029491596
20	1.182275371	14.296297373	5.145426921
20	1.184491282	14.292067804	12.031569390
20	0.013426395	5.417815277	3.421650414
20	-0.003480441	5.424296976	10.304540600
20	9.392709952	5.422883296	10.420105390
20	-4.707457213	13.548115140	3.421650414

20	-4.693390479	13.559516040	10.304540600
20	4.694030813	13.571370342	3.421650414
20	4.696870915	13.553487742	10.304540600
20	4.686702963	2.713442266	3.406618742
20	4.675865847	2.712256563	10.308786748
20	14.092158781	2.702082680	3.406618742
20	14.098604189	2.693290313	10.308786748
20	0.000000149	10.845767321	3.419955437
20	0.000000149	10.845767321	10.306157403
20	9.399268563	10.853126146	3.406618742
20	9.403660272	10.863104215	10.308786748
15	1.592135479	3.236254150	1.699876873
15	1.588607550	3.237954186	8.581877887
15	11.000240105	3.213018874	1.694281555
15	10.993639411	3.241307327	8.608808165
15	-3.112309593	11.367813163	1.703909799
15	-3.099934213	11.380225381	8.584439133
15	6.283774880	11.391381551	1.704343246
15	6.288611118	11.370975756	8.587745128
15	3.105906714	4.892760186	5.158182454
15	3.098123193	4.891763411	12.021727636
15	12.525314488	4.901528689	5.129507908
15	12.504341934	4.898241381	12.033897074
15	-1.592805141	13.026504010	5.145438636
15	-1.590695510	13.026796189	12.022509424
15	7.800403102	13.033752591	5.145957554
15	7.802222707	13.030174513	12.019704246
15	1.104050185	7.889404863	1.703909799
15	1.087113198	7.893916147	8.584439133
15	10.502744304	7.919977693	1.694281555
15	10.481546132	7.900117097	8.608808165
15	-3.614402874	16.014868519	1.704343246
15	-3.599149057	16.029259721	8.587745128
15	5.793964326	16.029353313	1.699876873
15	5.794256016	16.025448019	8.581877887
15	3.597657645	0.238471182	5.145957554
15	3.599846549	0.241836045	12.019704246
15	12.995212074	0.243414253	5.158182454
15	12.999967067	0.237171915	12.021727636
15	-1.092170729	8.375989376	5.145438636
15	-1.093478579	8.377670280	12.022509424
15	8.277914441	8.396476423	5.129507908
15	8.291247610	8.379957312	12.033897074
15	-2.669371583	5.131051413	1.704343246
15	-2.689461639	5.137066005	8.587745128
15	6.675145875	5.135654045	1.694281555
15	6.702944741	5.127226188	8.608808165
15	-7.386099383	13.271694019	1.699876873
15	-7.382863144	13.273899278	8.581877887
15	2.008259830	13.280083457	1.703909799
15	2.012821437	13.263159954	8.584439133
15	7.374900524	2.970645979	5.129507908
15	7.382539909	2.990452398	12.033897074
15	16.780068705	2.996427319	5.145957554
15	16.776060196	2.996640534	12.019704246
15	2.684975461	11.134808576	5.145438636
15	2.684173680	11.132835493	12.022509424
15	12.077010665	11.132476652	5.158182454
15	12.080039192	11.139715766	12.021727636
8	3.013423689	2.626621484	1.703892917
8	3.025577804	2.666314925	8.582842997
8	12.436858294	2.619060231	1.676557339
8	12.415821071	2.659924682	8.563007980
8	-1.677740573	10.786939067	1.708964229
8	-1.670381769	10.793344459	8.587364268
8	7.714292758	10.807266569	1.710733781
8	7.719829461	10.781689827	8.596601768
8	1.674727209	5.477061321	5.162547803
8	1.666799202	5.475294539	12.014690582
8	11.107690175	5.517371842	5.112932405

8	11.076770460	5.494202634	12.044149058
8	-3.023597445	13.612708505	5.145196690
8	-3.021791119	13.611693064	12.019283771
8	6.369667616	13.619778920	5.146186848
8	6.371051433	13.613958156	12.014986519
8	5.568905851	1.277140219	1.710733781
8	5.588287607	1.294723516	8.596601768
8	15.003986848	1.296390727	1.703892917
8	14.963534262	1.287069780	8.582842997
8	0.889816699	9.422215378	1.708964229
8	0.880590064	9.425385593	8.587364268
8	10.298817783	9.461105113	1.676557339
8	10.273946742	9.422454118	8.563007980
8	-0.884442975	6.843784402	5.145196690
8	-0.884466739	6.845856447	12.019283771
8	8.453390369	6.860855934	5.112932405
8	8.488915349	6.845663280	12.044149058
8	-5.587198664	14.975055361	5.146186848
8	-5.582849643	14.979164164	12.014986519
8	3.812071836	14.980476499	5.162547803
8	3.817565918	14.974494035	12.014690582
8	5.442453779	4.188485519	1.676557339
8	5.488362044	4.186272063	8.563007980
8	14.894931247	4.184244076	1.710733781
8	14.870012787	4.192237521	8.596601768
8	0.787923869	12.328147290	1.708964229
8	0.789791700	12.318571682	8.587364268
8	10.160719320	12.345638652	1.703892917
8	10.189017790	12.315266159	8.582842997
8	-0.782468929	3.942467437	5.146186848
8	-0.788201767	3.944179398	12.014986519
8	8.617049341	3.890423071	5.112932405
8	8.612444076	3.928784933	12.044149058
8	-5.486799022	12.079763898	5.162547803
8	-5.484365097	12.087513145	12.014690582
8	3.908040443	12.080808811	5.145196690
8	3.906257882	12.079752208	12.019283771
8	1.639971390	4.791875552	1.679557485
8	1.606503264	4.795217293	8.564982959
8	11.042872442	4.757855143	1.718575327
8	11.025565493	4.802722847	8.709577791
8	-3.086350131	12.924341416	1.687040970
8	-3.070845912	12.936575366	8.572799238
8	6.314336210	12.948468447	1.688744617
8	6.319259530	12.926438338	8.578013158
8	3.078485042	3.335836869	5.162907554
8	3.072763851	3.335403362	12.052191323
8	12.471700341	3.345462764	5.119199026
8	12.465631003	3.341856076	12.012112996
8	-1.620865344	11.470283176	5.148365753
8	-1.619218815	11.470289157	12.035286701
8	7.770516385	11.477680758	5.143671740
8	7.773875169	11.473730946	12.029518467
8	-0.256922968	7.133622534	1.687040970
8	-0.275269989	7.140932607	8.572799238
8	9.143560268	7.184480489	1.718575327
8	9.113357171	7.147058379	8.709577791
8	-4.978160760	15.262792203	1.688744617
8	-4.961543786	15.278070978	8.578013158
8	4.422838305	15.292969970	1.679557485
8	4.436678335	15.262314852	8.564982959
8	4.960198606	0.990624206	5.143671740
8	4.961939851	0.995507904	12.029518467
8	14.357257918	0.998127812	5.162907554
8	14.360493942	0.993389869	12.052191323
8	0.269586013	9.129798709	5.148365753
8	0.268757569	9.131221654	12.035286701
8	9.652313999	9.128077937	5.119199026
8	9.658472151	9.124625079	12.012112996
8	-1.336175440	4.326041077	1.688744617

8	-1.357715735	4.332792411	8.578013158
8	7.991697160	4.326315224	1.718575327
8	8.039207206	4.318869629	8.709577791
8	-6.062809686	12.452456204	1.679557485
8	-6.043181590	12.479769581	8.564982959
8	3.343273108	12.479337776	1.687040970
8	3.346115910	12.459793754	8.572799238
8	6.054115530	3.795110155	5.119199026
8	6.054026716	3.802169700	12.012112996
8	15.447414880	3.800345892	5.143671740
8	15.442314850	3.799412006	12.029518467
8	1.351279340	11.937219842	5.148365753
8	1.350461255	11.935790916	12.035286701
8	10.742386910	11.934686174	5.162907554
8	10.744872077	11.939857625	12.052191323
8	0.791335920	2.759860149	0.461458443
8	0.794533989	2.749912655	7.344862178
8	10.197206603	2.778733534	0.434800185
8	10.188433166	2.926186464	7.308698873
8	-3.903537969	10.886230828	0.463092702
8	-3.895455036	10.903957467	7.343287526
8	5.489933329	10.919947296	0.459888629
8	5.498650182	10.894617253	7.343127020
8	3.913139272	5.363908696	6.395719254
8	3.893886432	5.391146231	13.251286511
8	13.295423064	5.338232911	6.405760041
8	13.307220804	5.342325795	13.280755744
8	-0.797540898	13.491762952	6.391494427
8	-0.796426563	13.501355522	13.264862072
8	8.594982552	13.491887974	6.394971904
8	8.594042480	13.508501675	13.261266737
8	1.916726495	7.444972401	0.463092702
8	1.897333309	7.443109107	7.343287526
8	11.280362778	7.441673193	0.434800185
8	11.157051514	7.360348710	7.308698873
8	-2.809208471	15.563098941	0.459888629
8	-2.791630437	15.583312978	7.343127020
8	6.606933000	15.574037796	0.461458443
8	6.613948748	15.581781152	7.344862178
8	2.803610904	0.697529243	6.394971904
8	2.789693053	0.688408266	13.261266737
8	12.183569080	0.706923665	6.395719254
8	12.169607103	0.676631449	13.251286511
8	-1.892729049	8.832078707	6.391494427
8	-1.901593626	8.828247464	13.264862072
8	7.514663066	8.845057667	6.405760041
8	7.505219655	8.853228367	13.280755744
8	-2.680724849	6.054255490	0.459888629
8	-2.707019736	6.059371495	7.343127020
8	6.700560490	6.048244128	0.434800185
8	6.832645190	5.982115682	7.308698873
8	-7.398268911	14.203403782	0.461458443
8	-7.408482728	14.205607920	7.344862178
8	1.986811482	14.206098497	0.463092702
8	1.998121736	14.190235152	7.343287526
8	7.368043740	2.085360278	6.405760041
8	7.365689412	2.073096694	13.280755744
8	16.779536414	2.079233639	6.394971904
8	16.794394337	2.071740914	13.261266737
8	2.690269956	10.213460069	6.391494427
8	2.698020198	10.207698741	13.264862072
8	12.081421518	10.197818494	6.395719254
8	12.114636335	10.200873176	13.251286511
8	3.887512428	5.351600126	3.903380903
8	3.888531509	5.322696179	10.759529042
8	13.341356028	5.371557131	3.902582374
8	13.298815790	5.374791059	10.791014937
8	-0.799343166	13.491610357	3.899036591
8	-0.795774442	13.479015345	10.771482693
8	8.596028412	13.502477803	3.902051919

8	8.599820985	13.479670965	10.768915289
8	0.796146927	2.800666801	2.956692505
8	0.800845637	2.785402888	9.836732314
8	10.224064021	2.644252939	2.904088779
8	10.190358426	2.687340297	9.800994093
8	-3.905097518	10.921341229	2.958420986
8	-3.896358493	10.927820830	9.835460049
8	5.483642044	10.949220539	2.954825090
8	5.491756978	10.909922465	9.834278510
8	2.793916913	0.693140070	3.902051919
8	2.811771928	0.707827954	10.768915289
8	12.207042037	0.690884452	3.903380903
8	12.231564049	0.706218975	10.759529042
8	-1.891695765	8.830594194	3.899036591
8	-1.882572526	8.839982306	10.771482693
8	7.462836963	8.868174671	3.902582374
8	7.481306419	8.829716780	10.791014937
8	1.887099771	7.426066591	2.958420986
8	1.877118759	7.430395008	9.835460049
8	11.383397681	7.532172697	2.904088779
8	11.362935732	7.481439117	9.800994093
8	-2.831414201	15.543013907	2.954825090
8	-2.801438537	15.569690682	9.834278510
8	6.569187899	15.557800924	2.956692505
8	6.580057481	15.569502083	9.836732314
8	7.373936879	2.028919054	3.902582374
8	7.398007662	2.064143017	10.791014937
8	16.788184545	2.073032983	3.902051919
8	16.766536957	2.081151937	10.768915289
8	2.691038940	10.215097175	3.899036591
8	2.678346977	10.218304076	10.771482693
8	12.083575405	10.226166277	3.903380903
8	12.058034313	10.239735702	10.759529042
8	-2.652227834	6.045067281	2.954825090
8	-2.690318432	6.057688579	9.834278510
8	6.570668168	6.092225219	2.904088779
8	6.624835712	6.099871442	9.800994093
8	-7.365334817	14.178834002	2.956692505
8	-7.380903109	14.182396756	9.836732314
8	2.017997756	14.189893906	2.958420986
8	2.019239743	14.179085888	9.835460049
9	0.000000000	0.000000000	1.738408395
9	0.000000000	0.000000000	8.623174426
9	9.368964144	-0.022206717	1.706216244
9	9.401669970	0.004357270	8.563074720
9	-4.665250491	8.124864314	1.706216244
9	-4.704608491	8.139906397	8.563074720
9	4.688996306	8.165993263	1.706216244
9	4.695648481	8.124387194	8.563074720
9	0.000000000	0.000000000	5.159618466
9	0.000000000	0.000000000	12.016242934
9	9.389998044	0.001797504	5.161713745
9	9.390340366	-0.007000131	12.006902018
9	-4.696555706	8.131078096	5.161713745
9	-4.689107892	8.135773373	12.006902018
9	4.699267621	8.135775261	5.161713745
9	4.691477486	8.139877619	12.006902018

Cartesian coordinates – Ce2-Na1-close model

58	5.949762674	6.283992892	5.170646014
11	9.457141115	5.394556597	6.837662399
20	4.690593635	2.698998863	13.746677254
20	4.706174015	2.675373909	6.892851701
20	14.095107145	2.694079879	13.754263087
20	14.081919095	2.712384746	6.877786760
20	-0.006850761	10.846224930	13.749993443
20	-0.007430670	10.870594851	6.874958794
20	9.399672681	10.840626521	13.749491672
20	9.451012897	10.880939938	6.890862867
20	-0.016305431	5.420518629	6.860947242

20	-0.009695238	5.417159892	13.732378147
20	9.418821480	5.417153901	13.714934084
20	-4.714036973	13.539514466	6.852568347
20	-4.699598158	13.545279308	13.732362941
20	4.695883111	13.567891165	6.856619428
20	4.688267986	13.563651882	13.731131862
20	8.216936275	1.963127080	1.698558025
20	8.233055447	1.976293748	8.579271051
20	17.612815080	1.962521094	1.700982368
20	17.609214057	1.962788699	8.585970458
20	3.508595860	10.103855907	1.706322273
20	3.507821747	10.112663357	8.578245048
20	12.903950625	10.093401544	1.703904593
20	12.895297785	10.063093669	8.578421486
20	3.562221316	6.127005046	1.681538792
20	3.582423240	6.129718368	8.612552338
20	12.978155351	6.116015641	1.701508790
20	12.949059584	6.113569276	8.573146299
20	-1.122184858	14.250504561	1.697637402
20	-1.129724026	14.242917775	8.586186267
20	8.273457312	14.251649358	1.699046603
20	8.273609661	14.250390560	8.584115819
20	1.113501021	2.016497524	5.142921869
20	1.115601627	2.009172408	12.023592250
20	10.523613270	2.029815779	5.168845946
20	10.519022413	2.011843930	12.020407643
20	-3.601435959	10.134500149	5.140144267
20	-3.585006277	10.138408819	12.019397034
20	5.799521537	10.221258155	5.139765187
20	5.817889324	10.139313119	12.019554756
20	2.301935605	0.034575623	1.699782984
20	2.305401277	0.037661611	8.586748596
20	11.703343403	0.040472358	1.705710985
20	11.683390985	0.062210889	8.579589297
20	-2.400520896	8.168188933	1.692752461
20	-2.392838222	8.162748981	8.590607986
20	7.019073503	8.176004401	1.660062797
20	7.028488137	8.154700835	8.612954707
20	2.290029529	8.127560643	5.142125649
20	2.397803870	8.098059348	12.022002793
20	11.748890138	8.069159205	5.168684653
20	11.788207688	8.083032950	12.019872547
20	-2.311463863	16.221447673	5.142609432
20	-2.302345598	16.227017151	12.019049964
20	7.090457287	16.230647389	5.140713839
20	7.089092313	16.221835832	12.021139292
20	-3.518587071	6.161887237	5.142665214
20	-3.516907723	6.156778719	12.018285849
20	5.883223673	6.143523242	12.026109818
20	-8.217318415	14.306268922	5.140269152
20	-8.215349423	14.289663635	12.021914560
20	1.175774899	14.315035827	5.139693929
20	1.181132523	14.293551667	12.018837661
20	-0.022417840	5.423342976	3.416438430
20	-0.003052318	5.410604635	10.308126374
20	9.464348382	5.384357294	3.460090882
20	9.427246232	5.416016656	10.230489548
20	-4.701689058	13.549569893	3.420568299
20	-4.705574791	13.545726461	10.304735581
20	4.696840730	13.551963615	3.416622320
20	4.693036668	13.566263112	10.304440679
20	4.720107316	2.658115231	3.414624060
20	4.697165182	2.682117742	10.310604125
20	14.091429632	2.733469017	3.428293470
20	14.100398517	2.711463774	10.298216879
20	-0.009870390	10.872839340	3.416830306
20	-0.007256596	10.848653601	10.300223350
20	9.409905705	10.861296862	3.417161567
20	9.381863803	10.842892537	10.302301371
15	1.597443164	3.239923510	1.706312925

15	1.596086494	3.235377750	8.581219374
15	10.993761154	3.229506480	1.700778918
15	11.001996839	3.210303394	8.587568200
15	-3.113090703	11.366709201	1.701772310
15	-3.120699072	11.362920351	8.577984944
15	6.287535143	11.369921288	1.699979462
15	6.286948428	11.366592919	8.570617615
15	3.098862368	4.908237006	5.140221944
15	3.099372844	4.892320106	12.030601554
15	12.522069686	4.904411411	5.137507741
15	12.511126823	4.883119965	12.021062029
15	-1.604948551	13.028810002	5.141448171
15	-1.595845859	13.017236338	12.024066756
15	7.806114049	13.007758701	5.144175700
15	7.799588764	13.029316648	12.026511349
15	1.088594793	7.900897748	1.698742848
15	1.094100337	7.895634708	8.586086859
15	10.481426346	7.882019191	1.701587421
15	10.493668199	7.905646442	8.586864024
15	-3.611355697	16.011153795	1.692191188
15	-3.611695262	16.008024396	8.582005936
15	5.791698738	16.023471205	1.707356581
15	5.792530248	16.023047517	8.576815723
15	3.597665260	0.236977647	5.144401683
15	3.601998830	0.232486869	12.028905721
15	13.013826199	0.240626685	5.136308465
15	13.001182194	0.236487253	12.027245709
15	-1.123000311	8.379236584	5.140804897
15	-1.090773927	8.374327029	12.023209037
15	8.260205393	8.354624602	5.127907253
15	8.318422074	8.373003333	12.019416063
15	-2.678248653	5.128914141	1.694924579
15	-2.673587835	5.127444384	8.580782684
15	6.720674074	5.105314542	1.667318839
15	6.697533488	5.098734829	8.636368133
15	-7.389269062	13.270452944	1.698227827
15	-7.388736797	13.274162780	8.588341666
15	2.009664299	13.269934603	1.697024438
15	2.010717562	13.277796230	8.581983465
15	7.385759448	2.992774132	5.136850124
15	7.383864319	2.993168007	12.021759061
15	16.798546867	2.989062843	5.144468567
15	16.785151232	2.987303486	12.027666391
15	2.661088311	11.149559022	5.142139282
15	2.691141171	11.128870236	12.024241571
15	12.067138976	11.133567569	5.133245807
15	12.084412815	11.121282736	12.026781758
8	3.031849809	2.662496014	1.711450065
8	3.021375086	2.634971603	8.582779934
8	12.422734627	2.639968582	1.708151841
8	12.436632009	2.611012984	8.611353537
8	-1.681417751	10.782473024	1.707495872
8	-1.685116164	10.785427257	8.575983213
8	7.717842680	10.782618534	1.718711241
8	7.714094455	10.767633148	8.544865583
8	1.674042855	5.487442242	5.134489260
8	1.667909166	5.475692532	12.031859289
8	11.121834339	5.532534872	5.112409200
8	11.077799329	5.458068557	12.013174908
8	-3.033362383	13.621894734	5.139742599
8	-3.027209797	13.599335985	12.020409961
8	6.367825318	13.571593652	5.138278294
8	6.369845750	13.618066896	12.023417091
8	5.573189803	1.274399114	1.684846324
8	5.576225187	1.272325018	8.589908314
8	14.988035186	1.287878058	1.718171567
8	15.012227158	1.290513912	8.575653261
8	0.876412044	9.431119039	1.703390184
8	0.875761738	9.425929529	8.585513686
8	10.256335340	9.412789628	1.702389046

8	10.287561857	9.447625221	8.617042286
8	-0.858286083	6.856129838	5.138019990
8	-0.879216938	6.842935462	12.019852711
8	8.500533935	6.828975981	5.091977795
8	8.534470394	6.846025037	12.013663321
8	-5.603230559	14.971875119	5.137646605
8	-5.594831950	14.968172725	12.024728034
8	3.833438575	14.976079443	5.128694039
8	3.812893171	14.971506544	12.026286420
8	5.494585557	4.167768647	1.701855593
8	5.453253780	4.174255810	8.623430123
8	14.892308775	4.181554442	1.691846675
8	14.894940806	4.182763904	8.578392652
8	0.781592016	12.329812435	1.697425357
8	0.786595703	12.330644057	8.585153625
8	10.179526174	12.321690823	1.696595319
8	10.162855456	12.347524283	8.597908343
8	-0.773595122	3.945650678	5.140559422
8	-0.783418276	3.936785862	12.026233924
8	8.603229635	3.921703483	5.113348751
8	8.596512582	3.948479587	12.015604900
8	-5.486683129	12.061708725	5.127177300
8	-5.488156464	12.075699325	12.028692865
8	3.897239485	12.077548773	5.141140765
8	3.917329346	12.071841558	12.021554573
8	1.619142648	4.797711151	1.704355217
8	1.635736667	4.792300627	8.569925328
8	11.030387457	4.785595515	1.682275703
8	11.050416701	4.753955862	8.546068827
8	-3.081796750	12.923293288	1.695986321
8	-3.094144680	12.919855321	8.567394103
8	6.315902886	12.924985632	1.662202375
8	6.323016664	12.922418849	8.586419011
8	3.094254468	3.358704065	5.144332655
8	3.073995546	3.336540218	12.021631831
8	12.469626112	3.344809974	5.170094357
8	12.490599494	3.326091796	12.036856922
8	-1.640697689	11.472599505	5.151234332
8	-1.622351955	11.460608575	12.030986853
8	7.793544749	11.448752860	5.170179827
8	7.767272757	11.472675256	12.037902652
8	-0.268742161	7.141442084	1.681241485
8	-0.261713822	7.133072367	8.586739661
8	9.126131975	7.116099027	1.706726618
8	9.136513649	7.167732048	8.528778809
8	-4.972866104	15.256910287	1.692276198
8	-4.975335707	15.257042763	8.561965925
8	4.429306858	15.269901755	1.694579148
8	4.422316630	15.284984903	8.582650284
8	4.963024698	0.984386775	5.166055694
8	4.965776283	0.982183044	12.038837722
8	14.371451191	1.003567942	5.143508272
8	14.364761596	0.988819971	12.017879750
8	0.220847112	9.168974709	5.147679165
8	0.270764975	9.130104875	12.029030410
8	9.591144738	9.142620419	5.196215767
8	9.671214136	9.141046080	12.030899730
8	-1.345046387	4.323221977	1.683497290
8	-1.341687570	4.318457799	8.581675950
8	8.055376639	4.318197092	1.670220163
8	8.010306127	4.300311481	8.583122956
8	-6.058768602	12.463076005	1.697577734
8	-6.070668182	12.448165199	8.578551582
8	3.339754720	12.460142460	1.687352542
8	3.343644630	12.472126160	8.574848512
8	6.043557334	3.817244589	5.174465869
8	6.039491521	3.784430206	12.034803366
8	15.466526781	3.790703815	5.162811288
8	15.454278766	3.792535193	12.035373383
8	1.336315732	11.964421523	5.147846471

8	1.358063773	11.932734871	12.029277427
8	10.746769711	11.959074207	5.139004869
8	10.750325104	11.926217761	12.017438648
8	0.808520789	2.766496851	0.460311017
8	0.800910389	2.768898127	7.336839649
8	10.198433584	2.749339454	0.461805412
8	10.222793668	2.631896213	7.383227123
8	-3.904532145	10.895637884	0.456747784
8	-3.918837611	10.889496924	7.336851799
8	5.496199098	10.861023039	0.470299228
8	5.474462121	10.926551005	7.325781720
8	3.902292522	5.402725225	6.379136911
8	3.893411668	5.348394828	13.280979367
8	13.335222301	5.371992801	6.373887112
8	13.301281364	5.364305626	13.265602449
8	-0.806226100	13.499585457	6.383021148
8	-0.799937402	13.486115343	13.267876769
8	8.599306741	13.499327080	6.380406902
8	8.598170538	13.500846320	13.267156448
8	1.911364208	7.454158816	0.463136645
8	1.895891239	7.445399272	7.337930691
8	11.281698440	7.432629749	0.453332718
8	11.398256320	7.536969693	7.389403573
8	-2.805256597	15.554555125	0.451197734
8	-2.798387744	15.564208298	7.341519899
8	6.599533864	15.577037191	0.462675544
8	6.581595967	15.550283303	7.327943033
8	2.786199292	0.695351482	6.381776956
8	2.796993250	0.691668140	13.270816581
8	12.210490717	0.680280920	6.383291730
8	12.213762515	0.693720313	13.280081029
8	-1.937888575	8.806937771	6.383319533
8	-1.894074149	8.826960092	13.267874741
8	7.337790458	8.696458936	6.331588992
8	7.508354010	8.825028331	13.262660818
8	-2.685854596	6.057515898	0.454531273
8	-2.659134186	6.046483887	7.332856361
8	6.693734822	6.046980661	0.442561920
8	6.598024936	6.066756748	7.421832823
8	-7.396276009	14.192331953	0.453868891
8	-7.393506357	14.191544497	7.339052006
8	2.003590564	14.194347620	0.454249621
8	1.998977999	14.198294387	7.335950321
8	7.375456137	2.060157242	6.372616497
8	7.398833133	2.068675052	13.267748902
8	16.826418532	2.057204326	6.381151270
8	16.795774235	2.062625525	13.270551167
8	2.654076653	10.226966383	6.387416339
8	2.699559492	10.205616112	13.268890474
8	12.051598599	10.224615159	6.385457412
8	12.080341709	10.210086556	13.280009397
8	3.915646092	5.399326682	3.906829464
8	3.892532306	5.374099907	10.791760541
8	13.343907881	5.301910209	3.876781815
8	13.308801403	5.339032138	10.772456916
8	-0.809196587	13.480092123	3.889755551
8	-0.800017640	13.472559679	10.774709024
8	8.592044343	13.453950971	3.885717098
8	8.594233202	13.481873350	10.775779620
8	0.804217961	2.778086093	2.953562892
8	0.800729947	2.786076892	9.832398446
8	10.195989611	2.788566686	2.955173064
8	10.201571698	2.794094813	9.855094198
8	-3.911998118	10.911303024	2.949058049
8	-3.907426370	10.907246499	9.830866892
8	5.485980608	10.948784327	2.959168409
8	5.502164232	10.891502107	9.818321782
8	2.823882395	0.711152394	3.888261412
8	2.812973294	0.697354806	10.778346783
8	12.211552540	0.696607513	3.892735612

8	12.189605493	0.682718478	10.788213913
8	-1.925956143	8.814678045	3.892082830
8	-1.886007321	8.833314839	10.775167159
8	7.449965523	8.799163957	3.877635997
8	7.518406989	8.841033659	10.776465588
8	1.875029751	7.439768821	2.952534405
8	1.899872515	7.442104508	9.829533930
8	11.290883584	7.439531312	2.945626264
8	11.243674399	7.412248271	9.858144961
8	-2.817792393	15.565109645	2.945466854
8	-2.832871039	15.542389073	9.837313005
8	6.581887141	15.551503238	2.955458039
8	6.590104968	15.559458808	9.822730561
8	7.308624824	2.092226404	3.874742231
8	7.377715512	2.070482814	10.775874245
8	16.799163547	2.078157606	3.891206501
8	16.787598371	2.071093148	10.778336468
8	2.645992129	10.234980016	3.890232196
8	2.692535205	10.210913773	10.775290899
8	12.036053616	10.213823122	3.887388274
8	12.104168391	10.196241018	10.786356527
8	-2.662076321	6.038316254	2.950337091
8	-2.666966338	6.042432241	9.831228581
8	6.716120181	6.031714093	2.920162979
8	6.722787514	6.025219735	9.876936711
8	-7.393711745	14.189149599	2.946560053
8	-7.372641372	14.193355074	9.834754623
8	2.014511693	14.181512169	2.949720984
8	2.014760664	14.189517669	9.833042198
9	0.003997232	-0.003455785	1.720068551
9	0.004637052	-0.003827621	8.598089094
9	9.397444017	-0.008035196	1.725667339
9	9.381047151	-0.029513741	8.631852820
9	-4.696782100	8.129793992	1.710548879
9	-4.674084353	8.119434948	8.634997330
9	4.711456022	8.119953060	1.765715316
9	4.702729781	8.139484855	8.583836582
9	0.003771870	0.003547548	5.121795076
9	0.001013035	-0.001570374	12.020549187
9	9.386068946	0.016505967	5.121291348
9	9.397337978	-0.005943723	12.037734117
9	-4.737456042	8.132905115	5.124029893
9	-4.698895424	8.130266690	12.036505995
9	4.588834704	8.221495672	5.122210591
9	4.703157993	8.125902372	12.038515983

Cartesian coordinates – Ce1-Si-close model

58	9.427270083	5.364236686	6.929563874
14	11.023455998	3.219350261	8.620377598
20	9.394393069	5.416478035	3.363107743
20	5.864955817	6.153124530	5.121935832
20	4.699450849	2.701037191	13.760096296
20	4.685364991	2.693035449	6.870575216
20	14.095556873	2.702745577	13.753497404
20	14.090474238	2.677767682	6.901948511
20	-0.001510384	10.844393420	13.757205601
20	0.006002840	10.849826284	6.874343183
20	9.395775032	10.819946533	13.756256053
20	9.391555874	10.861092997	6.868036529
20	-0.010771013	5.422978443	6.858270949
20	-0.008926460	5.419048996	13.744185221
20	9.385669491	5.420158894	13.743352866
20	-4.692373517	13.557207789	6.858010735
20	-4.696765552	13.556895220	13.740573410
20	4.692988870	13.565016053	6.856595332
20	4.706155152	13.535072432	13.743608183
20	8.213590191	1.967989915	1.701372484
20	8.267200255	1.969864156	8.623468398
20	17.600087742	1.966797205	1.704671153
20	17.609876943	1.962749201	8.589844535

20	3.507389399	10.102789260	1.701063476
20	3.506950509	10.105333315	8.582174658
20	12.913690076	10.100784466	1.700133872
20	12.923708012	10.102346852	8.599041675
20	3.570221027	6.120128562	1.700763994
20	3.563976983	6.126998370	8.599550477
20	12.982665465	6.112664776	1.699479395
20	12.999043685	6.100194126	8.610767922
20	-1.121525300	14.256186151	1.700256473
20	-1.114771261	14.256697895	8.582436958
20	8.279372446	14.249111365	1.699744146
20	8.284286460	14.233034461	8.586584149
20	1.110088727	2.010901459	5.148294460
20	1.103608234	2.007557404	12.029370161
20	10.521464576	2.008100433	5.162153671
20	10.519364238	1.983106576	12.010712483
20	-3.579343434	10.148466822	5.146454907
20	-3.575170947	10.148892833	12.031471835
20	5.801896051	10.137844458	5.142466699
20	5.815799534	10.142630179	12.031546763
20	2.297287790	0.038163842	1.703166673
20	2.303106167	0.036536437	8.588380758
20	11.704506691	0.031136211	1.704026305
20	11.724797993	0.069241470	8.599435199
20	-2.395850522	8.168061893	1.701582232
20	-2.395545671	8.174341601	8.582779247
20	6.994578676	8.170070698	1.694725551
20	6.985874671	8.205917320	8.606503738
20	2.389189876	8.091642194	5.149049381
20	2.384920866	8.091484205	12.032491560
20	11.795716886	8.101035112	5.128435565
20	11.815862032	8.098176806	12.024842722
20	-2.305727934	16.222425876	5.142419484
20	-2.321872062	16.222862961	12.032787845
20	7.089578018	16.222599729	5.142873540
20	7.096462790	16.215551029	12.030343092
20	-3.504895927	6.167645011	5.145774346
20	-3.496214254	6.150780203	12.033084921
20	5.856162669	6.164475333	12.029915433
20	-8.214097846	14.287278068	5.142893160
20	-8.212535027	14.292117032	12.029754477
20	1.187761848	14.299743142	5.151071470
20	1.187382410	14.291694586	12.026249207
20	-0.000429909	5.425018093	3.425987891
20	-0.008664178	5.412667267	10.311683413
20	9.472599324	5.299240992	10.398987420
20	-4.697588271	13.547466770	3.424319252
20	-4.700761580	13.559616566	10.307646981
20	4.696591019	13.541603491	3.421936391
20	4.699631264	13.560993312	10.311163073
20	4.661878850	2.695166633	3.416860967
20	4.688313987	2.706199707	10.306708648
20	14.114766579	2.684556753	3.425953083
20	14.074370208	2.676406019	10.279906823
20	-0.002220600	10.847548212	3.420854810
20	0.005669990	10.851063274	10.304195927
20	9.397723254	10.865967778	3.414697210
20	9.397787570	10.851101555	10.307898368
15	1.582006502	3.234063766	1.699948250
15	1.586827262	3.237969050	8.586842781
15	10.989445136	3.236686338	1.700367943
15	-3.107605056	11.371118285	1.701022558
15	-3.102752475	11.378500261	8.586957872
15	6.290449647	11.362482454	1.703122593
15	6.286288739	11.357995814	8.582714786
15	3.099955821	4.905237232	5.151491236
15	3.090209132	4.883338829	12.034174884
15	12.526504020	4.878967093	5.122139670
15	12.526212422	4.895861873	12.049792657
15	-1.590210384	13.028581746	5.144478458

15	-1.589390802	13.028340696	12.025584404
15	7.800362458	13.009086561	5.143179970
15	7.808580186	13.010652781	12.030227132
15	1.093024517	7.894596392	1.703578822
15	1.086962046	7.891658488	8.588587377
15	10.499323334	7.896057897	1.697163354
15	10.481862592	7.907667650	8.613748166
15	-3.620341584	16.017221518	1.706138553
15	-3.604359350	16.030569893	8.582260816
15	5.790941152	16.009279458	1.698382410
15	5.825524866	16.009062210	8.586938823
15	3.600278943	0.236262061	5.145928624
15	3.590763167	0.237225531	12.031019159
15	12.997368016	0.226279689	5.135334536
15	13.018549678	0.221849064	12.052264845
15	-1.096996870	8.378262248	5.144309295
15	-1.099134679	8.376505216	12.027184996
15	8.310383204	8.385670046	5.125105216
15	8.295890153	8.352602018	12.020571760
15	-2.679737396	5.127695969	1.707926941
15	-2.691118511	5.139872416	8.584961220
15	6.693267953	5.133370706	1.696521734
15	6.663397443	5.144003271	8.611611389
15	-7.390753825	13.268806477	1.696776930
15	-7.383989176	13.268509386	8.584301780
15	2.004286114	13.266943017	1.701049360
15	2.027010016	13.269047364	8.586178780
15	7.342311991	2.994423579	5.119609697
15	7.361654819	2.986157971	12.050258059
15	16.779301370	2.995465227	5.147427485
15	16.783755713	2.984200787	12.031212286
15	2.687879460	11.128338147	5.145676228
15	2.689100470	11.123497822	12.026658789
15	12.094568629	11.117677830	5.152427973
15	12.083277666	11.134294435	12.032207197
8	3.012629053	2.646170298	1.696963377
8	3.016665768	2.648652408	8.591638185
8	12.424100730	2.664766235	1.712558287
8	12.493135366	2.534101999	8.569244459
8	-1.677688123	10.783565907	1.704242021
8	-1.670934515	10.795780665	8.588795002
8	7.719568317	10.771412316	1.705452274
8	7.720939314	10.776062798	8.586662768
8	1.669669318	5.492354077	5.151998804
8	1.659559088	5.469638947	12.032304292
8	11.076805259	5.439826357	5.080701210
8	11.101355012	5.507486208	12.069013150
8	-3.022096942	13.613648069	5.145204478
8	-3.020371046	13.616734202	12.021495386
8	6.375705281	13.606513946	5.141394127
8	6.375988184	13.589647016	12.024060769
8	5.562599931	1.280429364	1.714761697
8	5.577004433	1.294044973	8.590261462
8	14.978124402	1.273567166	1.700142542
8	15.073534780	1.279512232	8.595532457
8	0.887674670	9.427132346	1.705806161
8	0.877420662	9.423419184	8.589987213
8	10.291143990	9.427668823	1.711120764
8	10.253656526	9.430545948	8.561253803
8	-0.888316876	6.846130207	5.143717572
8	-0.891912298	6.843760866	12.026216912
8	8.554009836	6.854340718	5.095186446
8	8.480937978	6.815481765	12.009497545
8	-5.599522834	14.969530582	5.138791953
8	-5.592009171	14.972420339	12.025008430
8	3.807240285	14.960349119	5.123622867
8	3.830114415	14.956209145	12.055157580
8	5.469950227	4.189816295	1.709031836
8	5.449165260	4.200102630	8.549484913
8	14.898595255	4.169958659	1.713055944

8	14.869701381	4.202810387	8.590403743
8	0.781043945	12.320443067	1.703900000
8	0.800738279	12.325200000	8.586432275
8	10.179735539	12.317434088	1.694037708
8	10.187069473	12.316641573	8.589360287
8	-0.787521870	3.942768893	5.135936447
8	-0.794163171	3.946214546	12.036592261
8	8.543150880	3.975284912	5.070866032
8	8.594409312	3.918266307	12.082145629
8	-5.476098005	12.067601373	5.152501293
8	-5.489469683	12.086638609	12.030014681
8	3.917044089	12.066555780	5.148634293
8	3.918690654	12.061312354	12.023266092
8	1.615463360	4.790728372	1.691708543
8	1.615100829	4.794596230	8.570928383
8	11.011307411	4.796532175	1.665963949
8	11.055052324	4.871534678	8.698451281
8	-3.078233964	12.927412340	1.688196665
8	-3.077171022	12.934990612	8.583219329
8	6.324512764	12.918040713	1.691200000
8	6.312597563	12.912742864	8.577679784
8	3.065161941	3.348635555	5.164893347
8	3.067031837	3.327115977	12.047108425
8	12.506037584	3.327297219	5.147785140
8	12.472050376	3.342550563	12.016906702
8	-1.618952675	11.471933547	5.152550195
8	-1.620821407	11.471473286	12.030712475
8	7.763299550	11.452462969	5.150062064
8	7.782991039	11.453174627	12.045365287
8	-0.269471577	7.142376684	1.691666003
8	-0.273445601	7.135993650	8.585748010
8	9.133674792	7.145319559	1.667843316
8	9.128503785	7.137769761	8.768270109
8	-4.980013818	15.258567739	1.694691853
8	-4.965352563	15.271620194	8.578704256
8	4.432527630	15.249622197	1.692530680
8	4.444592983	15.290573723	8.575823721
8	4.964278411	0.985521107	5.157678942
8	4.950496661	0.994147275	12.035302405
8	14.361904753	0.975161315	5.180063520
8	14.377342745	0.980401815	12.022793730
8	0.264861107	9.132050948	5.151878791
8	0.263824117	9.129119350	12.031048526
8	9.661340788	9.153867384	5.124826264
8	9.667050337	9.091455257	12.009695896
8	-1.342467944	4.331081808	1.698450148
8	-1.363428922	4.326743213	8.581755113
8	8.028014062	4.329865762	1.673577227
8	7.989880235	4.338365052	8.772555388
8	-6.057649370	12.464490423	1.688727062
8	-6.050071011	12.466056736	8.570160343
8	3.337269702	12.460606266	1.688824835
8	3.359301550	12.460538200	8.582661512
8	6.005426368	3.788635838	5.118685189
8	6.041202824	3.812759472	12.022542332
8	15.449035567	3.801454603	5.177943806
8	15.448210337	3.781700851	12.010387695
8	1.357495325	11.936457735	5.146463373
8	1.358845857	11.932760692	12.035399273
8	10.763156748	11.924659140	5.157642719
8	10.745393511	11.929601946	12.048540158
8	0.784563490	2.760169707	0.459870640
8	0.793132865	2.759403516	7.345850715
8	10.194403819	2.740221908	0.467946346
8	10.119515580	2.937600827	7.257793306
8	-3.903366490	10.895403794	0.459413043
8	-3.897070549	10.909284904	7.342988793
8	5.494512693	10.887908890	0.461477177
8	5.499304001	10.878572498	7.338168388
8	3.903424665	5.387407132	6.386780946

8	3.887467158	5.364012683	13.273072585
8	13.267176643	5.399574412	6.375326141
8	13.327330443	5.321338005	13.305072024
8	-0.793911170	13.498761303	6.388176064
8	-0.797414547	13.492413168	13.272896979
8	8.603144279	13.466200945	6.388104490
8	8.599728119	13.492604165	13.270887255
8	1.902635190	7.443730753	0.461868888
8	1.889490218	7.439312121	7.344108934
8	11.322374312	7.456903919	0.462425026
8	11.119397565	7.379771523	7.291034846
8	-2.811338977	15.569332529	0.462403638
8	-2.803009094	15.577916194	7.335647798
8	6.601411242	15.557990058	0.456943773
8	6.617499156	15.537614023	7.340418564
8	2.793328724	0.692034994	6.387974049
8	2.784891665	0.684354000	13.275165579
8	12.156687602	0.659200945	6.360518711
8	12.239188131	0.693915170	13.304041363
8	-1.903710327	8.830034148	6.387608038
8	-1.898270314	8.829838881	13.275029774
8	7.516762707	8.786834139	6.391612983
8	7.515188216	8.814117264	13.278152555
8	-2.693388127	6.052433060	0.463680211
8	-2.689860467	6.059981196	7.337946711
8	6.672613552	6.064366168	0.459113527
8	6.840629506	5.969125424	7.297059529
8	-7.403626888	14.196892641	0.457180012
8	-7.403979017	14.194449823	7.342722959
8	1.987361570	14.192556532	0.459331684
8	2.027662530	14.185186531	7.338694163
8	7.381367505	2.116764059	6.391524993
8	7.329824483	2.076304237	13.304497058
8	16.814859953	2.057296354	6.379175092
8	16.780350370	2.073707011	13.285691590
8	2.687974294	10.205956083	6.391158167
8	2.694810261	10.200953410	13.271770450
8	12.101480354	10.187086532	6.393435363
8	12.098754397	10.201700453	13.269759867
8	3.888075150	5.357934266	3.895666420
8	3.878201036	5.336172626	10.780360217
8	13.319920399	5.344118042	3.880846340
8	13.317725291	5.393594270	10.817179089
8	-0.798852248	13.486522490	3.894315345
8	-0.792017451	13.483942335	10.777140796
8	8.600893660	13.455404241	3.892728450
8	8.604518710	13.455204914	10.776665648
8	0.794266300	2.779008729	2.954402342
8	0.793528046	2.791294912	9.840192370
8	10.193940614	2.808713221	2.961729834
8	10.131273051	2.707378773	9.887234505
8	-3.903567014	10.922307182	2.952927128
8	-3.898754901	10.916843223	9.835474587
8	5.492347595	10.914727949	2.953699105
8	5.496320624	10.886622459	9.829442089
8	2.814710623	0.706007697	3.894890552
8	2.794416043	0.692780424	10.782253909
8	12.236342508	0.703026580	3.873540071
8	12.197344457	0.654087270	10.815436270
8	-1.890959440	8.834948888	3.894531805
8	-1.896231066	8.835062746	10.780357613
8	7.488673374	8.829660735	3.894094331
8	7.483861709	8.831154301	10.791216668
8	1.880982312	7.430986644	2.954695310
8	1.885149403	7.433905601	9.836745832
8	11.272652809	7.421272188	2.954083644
8	11.423442896	7.542477086	9.776501820
8	-2.828837782	15.554243991	2.955425300
8	-2.803963717	15.573237186	9.828045047
8	6.585405823	15.555999840	2.950507428

8	6.600318098	15.524282364	9.839122292
8	7.361794913	2.060327829	3.888446570
8	7.362515083	2.061288526	10.810066805
8	16.752691229	2.088668130	3.888895333
8	16.821930786	2.052126430	10.795897129
8	2.690771287	10.208882530	3.898309905
8	2.681444479	10.206922039	10.777116736
8	12.096481779	10.204523136	3.900419080
8	12.078829192	10.228338864	10.776303639
8	-2.675449267	6.046288730	2.956423369
8	-2.686095314	6.062116053	9.830860335
8	6.715494744	6.046471917	2.949734569
8	6.518349290	6.145034930	9.771640531
8	-7.392836229	14.179231136	2.950702510
8	-7.378788719	14.179440719	9.837137626
8	2.009928782	14.179469110	2.952800229
8	2.031971410	14.181175542	9.838408546
9	-0.002241800	-0.000214714	1.725340951
9	0.002952414	-0.009617332	8.606672056
9	9.395818446	-0.000948387	1.729520370
9	9.418045520	-0.018922264	8.541326167
9	-4.696789487	8.131120692	1.725583996
9	-4.694090438	8.136489870	8.525842847
9	4.695737572	8.129961925	1.725091954
9	4.691577256	8.135378749	8.519611992
9	0.000120560	-0.009362929	5.123061362
9	0.000923296	-0.011054403	12.035535042
9	9.390227641	0.002633184	5.118416675
9	9.378863335	-0.019848575	12.057583479
9	-4.703032219	8.137338414	5.124476952
9	-4.684035485	8.135641273	12.036075597
9	4.696445997	8.125755753	5.129742237
9	4.686133451	8.137038694	12.027510103

Cartesian coordinates – Ce2-Si-close model

58	5.734951401	10.098389649	5.142576935
14	8.283720557	8.342271684	5.144817405
20	9.370090676	5.424408519	3.448190122
20	9.376116308	5.424321125	6.826188073
20	5.958904535	6.095079503	5.145518040
20	4.687826819	2.698758031	13.750127248
20	4.693408561	2.713379275	6.876911998
20	14.086877586	2.719733768	13.755360374
20	14.078150039	2.725585789	6.871931734
20	-0.004483200	10.854971840	13.754304664
20	-0.055058312	10.868976580	6.878993205
20	9.401377178	10.860903145	13.756694287
20	9.397537895	10.785581731	6.854300521
20	0.014423557	5.426747556	6.855233109
20	-0.002612375	5.427625894	13.731330630
20	9.392324608	5.425238117	13.738868836
20	-4.703039008	13.585914353	6.853416076
20	-4.701550119	13.570243142	13.731485624
20	4.693974238	13.627197860	6.872893959
20	4.679385812	13.595096052	13.718583764
20	8.208381147	1.969455574	1.698607485
20	8.207820740	1.970717912	8.587511429
20	17.598283938	1.985559755	1.700613090
20	17.598676748	1.986564493	8.585190103
20	3.502918287	10.137168770	1.666610328
20	3.503040495	10.139490917	8.620606575
20	12.895954836	10.115763145	1.705875617
20	12.895404060	10.115265608	8.579450927
20	3.592378081	6.131338424	1.715461938
20	3.593729285	6.132664897	8.571564789
20	12.964795464	6.122156302	1.705056385
20	12.965728158	6.122524923	8.581146015
20	-1.125533982	14.271412801	1.699183832
20	-1.126363498	14.271457584	8.586478453
20	8.282877764	14.286484203	1.695790928

20	8.281967283	14.286790469	8.587512083
20	1.111147533	2.012214701	5.142229079
20	1.117317294	2.019883362	12.023269433
20	10.498734633	1.998958040	5.143006728
20	10.502392582	2.020479641	12.023694814
20	-3.608801400	10.146471479	5.143128709
20	-3.584417612	10.155539142	12.023784740
20	5.829724306	10.152704110	12.024821781
20	2.299798305	0.033865710	1.703537355
20	2.299095751	0.033813641	8.582291263
20	11.679769298	0.050821382	1.700912110
20	11.678379959	0.050974113	8.583781769
20	-2.400209037	8.180037214	1.699521768
20	-2.399993643	8.180397856	8.584887906
20	7.005698233	8.159906932	1.706976495
20	7.007247986	8.159851094	8.582361993
20	2.333618655	8.058570229	5.143412125
20	2.394066657	8.105678038	12.024728846
20	11.744980291	8.124179967	5.142734421
20	11.778745130	8.102223051	12.023348118
20	-2.311741993	16.228621618	5.143044527
20	-2.303845052	16.251380042	12.023506532
20	7.089237382	16.262794899	5.142181351
20	7.092663027	16.260054547	12.023778017
20	-3.522024580	6.161214078	5.142379071
20	-3.516550635	6.165807477	12.023822169
20	5.877344733	6.160489197	12.024338781
20	-8.206858611	14.312818189	5.142718458
20	-8.207718599	14.312494268	12.023460623
20	1.188438672	14.286001500	5.141985182
20	1.170354424	14.317818613	12.023708919
20	0.015753271	5.429512925	3.419700330
20	-0.001450695	5.430764184	10.304500599
20	9.389872324	5.423139910	10.298130766
20	-4.703908823	13.583478842	3.421676630
20	-4.703012047	13.568593929	10.304434465
20	4.694156830	13.625243939	3.402250020
20	4.680280542	13.593640137	10.317007058
20	4.693874425	2.709986729	3.417361005
20	4.688944464	2.698799826	10.306511351
20	14.077687079	2.726605634	3.422587932
20	14.086177419	2.718887402	10.301044186
20	-0.057583087	10.868551365	3.415022847
20	-0.004861943	10.854874059	10.302402438
20	9.400025001	10.788047212	3.439834151
20	9.401111835	10.864171899	10.299807744
15	1.593556942	3.249957713	1.698609150
15	1.594174964	3.250597214	8.585199357
15	10.981621107	3.236108127	1.700987992
15	-3.113852272	11.386291371	1.696416922
15	-3.113639775	11.385621730	8.587491742
15	6.298935807	11.432346872	1.657619637
15	6.297922609	11.433065262	8.627658160
15	3.121402886	4.871303659	5.144758518
15	3.102449252	4.913612448	12.024474613
15	12.494870077	4.888480456	5.143014920
15	12.494766112	4.888194055	12.024613858
15	-1.598775325	13.035054179	5.143629922
15	-1.598132764	13.040015074	12.024041315
15	7.794049718	13.071192034	5.142867346
15	7.799087546	13.052104237	12.023549962
15	1.097716357	7.907654937	1.708305023
15	1.097976446	7.907301613	8.576158763
15	10.489814252	7.888091920	1.697987276
15	10.489852920	7.888175351	8.586822062
15	-3.606799987	16.039373642	1.697425826
15	-3.608117324	16.038983844	8.586699983
15	5.785904736	16.062409308	1.698273974
15	5.785554161	16.061709157	8.585577848
15	3.596372196	0.243111739	5.143507247

15	3.593371941	0.237504864	12.024227243
15	12.993994593	0.252159736	5.142777067
15	12.982761335	0.249139775	12.023813036
15	10.982361059	3.236756575	8.583035280
15	-1.084091654	8.398747146	5.143180789
15	-1.096499439	8.386343563	12.024495239
15	8.304431640	8.389038642	12.025512934
15	-2.680701452	5.148364809	1.704246801
15	-2.681672325	5.148703294	8.579779543
15	6.699795406	5.120845294	1.681138299
15	6.701340678	5.119968389	8.605417136
15	-7.383494177	13.281861066	1.708182500
15	-7.384456943	13.281648099	8.575193676
15	2.004366390	13.289832581	1.700434952
15	2.003099512	13.290755531	8.582651084
15	16.781018560	3.004732916	5.143223344
15	7.373404367	2.999353564	12.025408983
15	7.400498332	2.948548694	5.144320121
15	16.770843676	3.005707426	12.023763584
15	2.710081028	11.133494263	5.144326361
15	2.669644252	11.159977588	12.025027459
15	12.077112630	11.161035999	5.143708602
15	12.075820863	11.143438305	12.024246554
8	3.018069601	2.649967267	1.702671589
8	3.018799752	2.651098242	8.587929134
8	12.415550393	2.653803323	1.698639416
8	12.415632152	2.653081819	8.592780681
8	-1.681113283	10.800563039	1.692188622
8	-1.680352711	10.801466595	8.598867495
8	7.720049632	10.844726662	1.685793833
8	7.719168176	10.845590114	8.608402644
8	1.697770231	5.481724153	5.144029486
8	1.669847103	5.500004884	12.022530235
8	11.072204720	5.486681826	5.139117718
8	11.062660431	5.467098986	12.021783457
8	-3.013121705	13.653801100	5.141600271
8	-3.028828373	13.625168429	12.021416831
8	6.342789223	13.606894107	5.140678159
8	6.367245203	13.639995365	12.020680807
8	5.580000497	1.281853652	1.705333690
8	5.579023330	1.281397038	8.585400160
8	14.979719618	1.305798051	1.714104284
8	14.980173037	1.305271259	8.577840155
8	0.897597349	9.442956434	1.736139838
8	0.896980883	9.442550664	8.557585110
8	10.276436152	9.420504557	1.691600609
8	10.275760227	9.420505109	8.600367800
8	-0.847120782	6.871837917	5.141239745
8	-0.886742137	6.854914075	12.022082194
8	8.446305880	6.725165927	5.143786763
8	8.525193048	6.860064305	12.023809214
8	-5.581479706	15.000863020	5.141408534
8	-5.598523193	14.993466128	12.022023090
8	3.812312311	15.008611663	5.140025804
8	3.793497206	15.004017268	12.020693654
8	5.480943929	4.169120517	1.677248747
8	5.483689702	4.167171655	8.618905011
8	14.879954075	4.196381027	1.707576545
8	14.879151057	4.196414711	8.583484648
8	0.788991372	12.333454471	1.710789561
8	0.788503979	12.333342971	8.579139377
8	10.180431509	12.327052367	1.720795656
8	10.179587433	12.326668813	8.568364931
8	-0.784627451	3.965236178	5.140494321
8	-0.789447411	3.958305777	12.020724007
8	8.635893811	3.873735306	5.142414111
8	8.591437650	3.951153436	12.023760534
8	-5.481739669	12.116444524	5.142516048
8	-5.482811924	12.093832499	12.022913717
8	3.889189905	12.142634569	5.143263306

8	3.887014022	12.110307300	12.022324787
8	1.632950223	4.807258781	1.680558908
8	1.632698180	4.807898957	8.580283574
8	11.008855319	4.791277049	1.700753479
8	11.010750463	4.791561317	8.556120595
8	-3.080440403	12.942216103	1.688893661
8	-3.081406080	12.941483197	8.567236700
8	6.316347861	12.984523550	1.634376077
8	6.315184154	12.985362431	8.619520172
8	3.069307270	3.315362534	5.145878165
8	3.071481206	3.356045165	12.030647060
8	12.454973268	3.331230029	5.151854799
8	12.470798886	3.331163702	12.031738271
8	-1.657423460	11.479472007	5.150370885
8	-1.624610479	11.483065423	12.032320120
8	7.783375148	11.508006980	5.149523619
8	7.771525835	11.495334994	12.034110745
8	-0.265180485	7.158370337	1.669846863
8	-0.265034436	7.156864677	8.583052015
8	9.128217925	7.133408616	1.706235004
8	9.129278321	7.132654404	8.556116577
8	-4.970828402	15.289372333	1.676237483
8	-4.972097157	15.288486870	8.584108761
8	4.418601620	15.315482942	1.658338955
8	4.417674794	15.314833122	8.603056733
8	4.957925335	0.996844700	5.150500892
8	4.958689491	0.985481483	12.031024193
8	14.355455748	1.007059590	5.150151038
8	14.349321279	0.994860541	12.032024325
8	0.271865924	9.171615871	5.150602846
8	0.266913398	9.140083428	12.033635280
8	9.696144705	9.164544687	5.147128665
8	9.661490383	9.151797439	12.030150389
8	-1.345519470	4.347437335	1.690998855
8	-1.346440686	4.347789283	8.569712118
8	8.035960028	4.323402163	1.693979407
8	8.037429286	4.323722261	8.556743994
8	-6.044862964	12.485944500	1.686343948
8	-6.045480793	12.485797763	8.570057431
8	3.343147369	12.494917029	1.677737543
8	3.342645269	12.496764170	8.581738403
8	6.074619632	3.766188472	5.150059445
8	6.034825445	3.794556809	12.033956166
8	15.443711618	3.800534237	5.150691747
8	15.436289415	3.805927066	12.031050456
8	1.352709639	11.881109110	5.146475165
8	1.333072458	11.955893634	12.032080251
8	10.740348213	11.957164144	5.151291390
8	10.743758976	11.949959389	12.030827205
8	0.794036076	2.777833463	0.457598192
8	0.797156833	2.787464617	7.339626492
8	10.188255396	2.765746990	0.455048127
8	10.192410303	2.733230443	7.350452730
8	-3.908459832	10.911859730	0.455379543
8	-3.898219193	10.897183674	7.345644468
8	5.489670642	10.923294742	0.442695103
8	5.487512336	10.991887690	7.372476470
8	3.918076209	5.312045801	6.396927513
8	3.893654293	5.387527383	13.268764343
8	13.297739377	5.346855791	6.387767767
8	13.290050324	5.358263535	13.269260319
8	-0.789038080	13.478833025	6.389293272
8	-0.803947556	13.512321239	13.268043687
8	8.572382318	13.553155666	6.385971713
8	8.594677651	13.526409532	13.265195537
8	1.929036954	7.479896415	0.474427777
8	1.892284165	7.434246709	7.331418364
8	11.283075084	7.431458643	0.446933747
8	11.322362975	7.456264141	7.355177431
8	-2.791165960	15.592333402	0.457977804

8	-2.806969008	15.576434095	7.343094780
8	6.615939023	15.625433238	0.466709058
8	6.561882958	15.588036296	7.329705974
8	2.789510311	0.691485532	6.387716049
8	2.791778703	0.697293246	13.267959912
8	12.189894581	0.697966304	6.388609363
8	12.177798632	0.698833641	13.267346822
8	-1.889795766	8.846851338	6.387776248
8	-1.901614308	8.840960268	13.267468184
8	7.399032532	8.877693254	6.437822282
8	7.497891255	8.840375652	13.270310153
8	-2.698009881	6.073168057	0.460936826
8	-2.695633544	6.075371220	7.337241559
8	6.702996796	6.043915603	0.436367240
8	6.642208471	6.059495518	7.379053441
8	-7.412436710	14.211865640	0.467551045
8	-7.394893010	14.213484315	7.336510079
8	1.973752111	14.220446155	0.463199394
8	1.997421607	14.210703846	7.334899104
8	7.397974360	2.028431137	6.389865734
8	7.387789955	2.071909430	13.267090201
8	16.799477365	2.079289409	6.385644162
8	16.783033533	2.083018187	13.267720632
8	2.814385818	10.197314104	6.375153687
8	2.678063813	10.233957412	13.266624446
8	12.103131860	10.238810619	6.387744250
8	12.084659435	10.220130716	13.268081650
8	3.917349315	5.312193285	3.891693973
8	3.893763183	5.376957477	10.775407747
8	13.297733074	5.331177237	3.891968500
8	13.289773396	5.346299286	10.774846028
8	-0.790728107	13.467031938	3.891976253
8	-0.804411668	13.497684138	10.773755076
8	8.572511451	13.542289612	3.894888024
8	8.593692672	13.507745478	10.773591213
8	0.796402038	2.810675282	2.952652360
8	0.794522694	2.801129634	9.834707037
8	10.191321166	2.760318144	2.944512288
8	10.187976363	2.796381209	9.839558870
8	-3.898510652	10.928241766	2.950072825
8	-3.908018189	10.939843327	9.839463484
8	5.489317995	11.022770483	2.924000315
8	5.488483208	10.955339858	9.855319904
8	2.800528604	0.696183051	3.893404909
8	2.802401515	0.702438276	10.775119840
8	12.201239665	0.704735838	3.891634471
8	12.190053218	0.706177620	10.774405565
8	-1.877628516	8.852080928	3.892013389
8	-1.886747477	8.847572088	10.773826221
8	7.401429418	8.879173640	3.850068285
8	7.505276289	8.844789422	10.776857735
8	1.863513365	7.418172871	2.964684820
8	1.901994485	7.464369194	9.822833502
8	11.302010352	7.442732186	2.938306127
8	11.263330097	7.419882024	9.845862867
8	-2.827279114	15.565095385	2.950376941
8	-2.814419044	15.579045281	9.835830043
8	6.542837175	15.576358229	2.961349343
8	6.595981280	15.612199639	9.825902080
8	7.389975353	2.034461745	3.893535787
8	7.376276413	2.081874328	10.775647871
8	16.788713129	2.085606991	3.895584151
8	16.772128465	2.088619700	10.775132456
8	2.811219679	10.198597571	3.911270581
8	2.667628001	10.240209261	10.778050215
8	12.093149587	10.248016689	3.892165837
8	12.075583962	10.227287521	10.774768747
8	-2.672015531	6.062930728	2.955912172
8	-2.676723405	6.061709148	9.832151148
8	6.672921314	6.042266271	2.922465047

8	6.736009005	6.024036612	9.863713398
8	-7.369712726	14.199000307	2.957982039
8	-7.389068460	14.196738956	9.827276013
8	2.020757769	14.197622966	2.957021876
8	1.992599983	14.209467305	9.829179808
9	0.000258552	0.013472406	1.740171102
9	-0.000846347	0.013550218	8.600672388
9	9.383396870	-0.010093879	1.727026751
9	9.382014601	-0.009151215	8.616047179
9	-4.695429777	8.143217416	1.719295195
9	-4.695048482	8.143292487	8.622609754
9	4.691542480	8.173600453	1.762221144
9	4.692731110	8.175106380	8.590658008
9	-0.000796403	0.002794483	5.144012845
9	0.004373728	0.004679679	12.023106744
9	9.396634280	-0.041938025	5.144337329
9	9.387473005	0.000418346	12.023649966
9	-4.701352644	8.132627953	5.141547163
9	-4.697616427	8.139793174	12.024816677
9	4.632022295	7.989961681	5.152073704
9	4.694880289	8.153170041	12.026040503

Cartesian coordinates – Ce2-Si-far

58	5.666163928	10.134048668	5.142891347
14	3.604722650	0.224433887	12.027268034
20	9.392047094	5.393806736	3.418483811
20	9.387394549	5.393269192	6.865059213
20	5.905828791	6.045745827	5.145327138
20	4.645241025	2.609033616	13.722484099
20	4.668737322	2.701594288	6.883447357
20	14.088316996	2.716008432	13.753236962
20	14.082872863	2.732740845	6.870689625
20	-0.004908866	10.862746579	13.751191628
20	-0.063370718	10.863484974	6.880608818
20	9.422043350	10.870933418	13.745670271
20	9.432346860	10.867571963	6.883842303
20	-0.001935909	5.427945660	6.858697509
20	-0.001507131	5.417011251	13.735649277
20	9.394413055	5.419363893	13.734399524
20	-4.697622430	13.592828592	6.861613830
20	-4.726381145	13.607324889	13.706413205
20	4.684155189	13.646574095	6.881214790
20	4.687345479	13.593775219	13.718888390
20	8.205693214	1.963675376	1.690838834
20	8.205883891	1.962694774	8.597731736
20	17.602405403	2.000168832	1.695638628
20	17.600949198	1.999271476	8.593336310
20	3.494061808	10.116136898	1.657877490
20	3.495091296	10.115737279	8.630830182
20	12.898310420	10.122755473	1.697985022
20	12.899221351	10.122668904	8.588486711
20	3.588852537	6.124061355	1.710466032
20	3.587279158	6.121324366	8.582772852
20	12.975457969	6.130434402	1.701811363
20	12.975242430	6.129652796	8.586794362
20	-1.134400975	14.272249067	1.694204634
20	-1.133925736	14.270318043	8.591576560
20	8.289791834	14.293480711	1.687879875
20	8.288902961	14.292832867	8.593642514
20	1.108365849	2.005142621	5.142202946
20	1.194552893	1.974783184	12.024623669
20	10.491863404	1.992127105	5.143610458
20	10.481034576	2.010963787	12.025622249
20	-3.591571477	10.160287959	5.142599106
20	-3.580148606	10.167557109	12.023365816
20	5.830747322	10.154727950	12.026216044
20	2.302916759	0.053659714	1.665782651
20	2.302171507	0.053585099	8.623334132
20	11.684077728	0.037331657	1.697331269
20	11.684500976	0.037086822	8.589467741

20	-2.399596130	8.192232042	1.693034310
20	-2.399461034	8.191450882	8.590078767
20	7.009746442	8.139930407	1.669913383
20	7.009266715	8.138690095	8.617142459
20	2.342314832	8.044092681	5.146998242
20	2.402729378	8.088911383	12.027970360
20	11.781021530	8.106798333	5.144389680
20	11.779848712	8.095925852	12.025345985
20	-2.306131251	16.241809574	5.142910885
20	-2.338139468	16.276672990	12.024758570
20	7.069822873	16.283692273	5.141945036
20	7.093309185	16.271880404	12.023727351
20	-3.525128713	6.168913465	5.143695943
20	-3.511026199	6.174376346	12.025177510
20	5.873052344	6.147207967	12.026080948
20	-8.214120852	14.329759223	5.143020484
20	-8.147760497	14.359471199	12.024911737
20	1.185440062	14.284576174	5.141992167
20	1.172039376	14.317271537	12.023612285
20	0.003963284	5.436319141	3.423941338
20	0.002723323	5.425819213	10.310178521
20	9.398461700	5.420330910	10.311934732
20	-4.699537480	13.590694814	3.419020058
20	-4.730235817	13.608052505	10.337418764
20	4.686980039	13.638586790	3.399995548
20	4.690790179	13.587900234	10.324118408
20	4.667130890	2.699097452	3.408333251
20	4.643514852	2.606291552	10.331927737
20	14.080565744	2.732218779	3.421118262
20	14.086080671	2.716936571	10.302689731
20	-0.070673503	10.864509184	3.410337729
20	-0.008665344	10.861193008	10.302912523
20	9.430621276	10.872508647	3.409119764
20	9.419602204	10.876177952	10.309776668
15	1.580060026	3.280445053	1.712344865
15	1.578615654	3.278971570	8.572386013
15	10.989475506	3.243819796	1.706320351
15	10.989499037	3.242937347	8.579388750
15	-3.119467575	11.386139970	1.697635458
15	-3.118782309	11.385716382	8.584686065
15	6.307042229	11.409150481	1.663695511
15	6.306869723	11.406818724	8.621517586
15	3.101893002	4.951909193	12.027924618
15	12.482151207	4.895273055	5.145333874
15	12.495644280	4.899531451	12.026602929
15	-1.595199439	13.032495875	5.143323282
15	-1.590004432	13.041503267	12.024055722
15	7.784418631	13.018434788	5.143303283
15	7.814758312	13.053152850	12.023896794
15	1.099580108	7.916480133	1.717330621
15	1.099117686	7.914166651	8.573019305
15	10.486445635	7.896797337	1.708736656
15	10.486522881	7.896434728	8.579028352
15	-3.602145953	16.038651082	1.716986867
15	-3.600394998	16.037721488	8.568317123
15	5.784712125	16.056114271	1.704251730
15	5.785250113	16.056757192	8.580637547
15	3.596413966	0.242142312	5.144491872
15	3.106201258	4.879913650	5.146267474
15	12.987190621	0.253572681	5.142539849
15	12.977183968	0.242868116	12.024255005
15	-1.079038527	8.399728114	5.143122501
15	-1.086131821	8.392958471	12.024705956
15	8.276106610	8.361162227	5.142914635
15	8.303025945	8.386717087	12.025006051
15	-2.695729794	5.162442600	1.707651985
15	-2.695365495	5.161384196	8.580078934
15	6.702181887	5.115939133	1.697140647
15	6.702955170	5.114663792	8.594213562
15	-7.388368992	13.290518351	1.720740155

15	-7.389581418	13.291493011	8.563922789
15	2.017663510	13.275025922	1.705909399
15	2.019726808	13.274286950	8.578966381
15	7.392309918	2.965641475	5.144045903
15	7.390774583	3.008037048	12.025499812
15	16.768293973	3.010121328	5.143223067
15	16.756306321	3.017618643	12.025060753
15	2.715761808	11.127459600	5.144902117
15	2.684001768	11.151448173	12.025716152
15	12.067171327	11.154099696	5.144611649
15	12.081918160	11.129188710	12.025138132
8	3.008298627	2.700085497	1.727672711
8	3.007442128	2.699884577	8.558937440
8	12.418934516	2.653720014	1.711074329
8	12.418853635	2.652367414	8.577775233
8	-1.684067087	10.803060480	1.695294612
8	-1.682470464	10.804926689	8.589881611
8	7.725562242	10.808785797	1.704157075
8	7.725795578	10.807096894	8.586701646
8	1.687448430	5.497267939	5.147538846
8	1.665034603	5.535444133	12.029273853
8	11.054725298	5.491271760	5.145558338
8	11.068239850	5.494442394	12.026029718
8	-3.015608217	13.632350854	5.141951916
8	-3.012560064	13.636981483	12.021962907
8	6.335481867	13.550750194	5.141684930
8	6.381798712	13.646276180	12.021739097
8	5.594056486	1.277516824	1.731512514
8	5.598164198	1.277043827	8.558763066
8	14.978096657	1.292843533	1.723081538
8	14.980713030	1.293786556	8.567455922
8	0.897951112	9.453034278	1.740677699
8	0.897922040	9.450729627	8.556939181
8	10.260380970	9.426810618	1.709132451
8	10.261120556	9.426491176	8.585168053
8	-0.859758321	6.871010241	5.142374142
8	-0.885833432	6.861179224	12.024227698
8	8.484603107	6.838798450	5.141018139
8	8.517578595	6.857653291	12.024863024
8	-5.595360923	15.001989364	5.142024514
8	-5.642725633	14.890632191	12.025833685
8	3.831240687	15.019100787	5.139078789
8	3.793004109	15.002530185	12.020366451
8	5.480698477	4.175408901	1.692665652
8	5.480941566	4.174688163	8.602332102
8	14.865932212	4.207190291	1.707228687
8	14.865700668	4.206972572	8.585673310
8	0.799128344	12.325279827	1.718205340
8	0.801230210	12.324265381	8.568903265
8	10.177329707	12.326197463	1.719020544
8	10.175871074	12.327472702	8.569048603
8	-0.798702783	3.968251141	5.140797237
8	-0.818665637	3.982003860	12.021509248
8	8.576727187	3.961728261	5.143920897
8	8.603030668	3.978303344	12.024365948
8	-5.485867796	12.091898110	5.143136638
8	-5.437563328	12.019841470	12.023243828
8	3.893853802	12.143481269	5.146240897
8	3.911842375	12.092547453	12.025362867
8	1.614485528	4.840053501	1.719273809
8	1.612303243	4.838577104	8.561871991
8	11.020040826	4.801013815	1.691428548
8	11.020426358	4.800204818	8.579553092
8	-3.086669699	12.939508953	1.682471647
8	-3.087541553	12.939196767	8.589185813
8	6.323853937	12.959829392	1.646316106
8	6.322940446	12.957743208	8.614978539
8	3.053422598	3.327471255	5.144233674
8	3.076177864	3.401850083	12.027200973
8	12.448213729	3.339197066	5.147921773

8	12.458213931	3.343023964	12.031782985
8	-1.640827565	11.475600228	5.148892451
8	-1.623831240	11.483271975	12.029040309
8	7.772197424	11.447374525	5.152502520
8	7.777175129	11.493620610	12.034301927
8	-0.263123974	7.167468039	1.683611776
8	-0.264374100	7.165783759	8.576435509
8	9.128985418	7.132388680	1.713756972
8	9.129004377	7.132566422	8.558141403
8	-4.965364650	15.289605143	1.702801312
8	-4.965141607	15.291204217	8.574489387
8	4.417654307	15.307878134	1.660450912
8	4.417519818	15.309908235	8.622148217
8	4.963689996	0.987942962	5.148587493
8	5.042394928	1.016003704	12.029726087
8	14.339789145	1.023742532	5.146460061
8	14.341586458	0.991585187	12.028332404
8	0.283566517	9.161679464	5.149149844
8	0.279161788	9.143414116	12.032660104
8	9.621229734	9.129362295	5.146523406
8	9.658997710	9.148270375	12.027067379
8	-1.362926815	4.361703997	1.712057534
8	-1.363076988	4.359985570	8.569346260
8	8.041808234	4.322341352	1.688074589
8	8.042333552	4.320775223	8.594892285
8	-6.053538641	12.490290115	1.695287696
8	-6.054843922	12.490489865	8.573815263
8	3.355903246	12.476218188	1.682159340
8	3.358164706	12.475862244	8.596937421
8	6.036971105	3.733555503	5.146640787
8	6.050190446	3.794606435	12.026946965
8	15.432684341	3.811346976	5.145650208
8	15.415154449	3.812628133	12.029423618
8	1.357552767	11.862619160	5.140890574
8	1.354600910	11.956976628	12.025492324
8	10.733651576	11.959781590	5.148656093
8	10.774541682	11.974696945	12.029560347
8	0.781035086	2.842423248	0.459868094
8	0.774922749	2.814405808	7.328132482
8	10.197143779	2.764597368	0.466459429
8	10.192842586	2.786653971	7.330739819
8	-3.913105672	10.888413277	0.467209313
8	-3.901998487	10.919924239	7.330484270
8	5.498924924	10.898716477	0.451906467
8	5.499976216	10.953306737	7.366213998
8	3.910769532	5.327014557	6.393395095
8	3.888672823	5.439696079	13.269662683
8	13.281722846	5.357931372	6.389606762
8	13.290596769	5.368853212	13.271117534
8	-0.785405201	13.478166670	6.388996793
8	-0.787917493	13.495135122	13.271746351
8	8.567794027	13.487182495	6.388785436
8	8.606639680	13.516657120	13.269840517
8	1.934866563	7.493188774	0.486266065
8	1.899784947	7.449505329	7.330044575
8	11.286915146	7.448308379	0.462510130
8	11.301444293	7.459062879	7.337147874
8	-2.783710298	15.595173562	0.479172066
8	-2.810509562	15.560749545	7.319983732
8	6.612907635	15.615844448	0.472778175
8	6.535065010	15.563776489	7.313413473
8	2.795433255	0.700642607	6.390167459
8	2.774687630	0.764067426	13.336820182
8	12.179034899	0.687500061	6.389476079
8	12.174974112	0.691287566	13.270052565
8	-1.880861854	8.854478580	6.388145727
8	-1.888690117	8.850903450	13.268559663
8	7.440599884	8.817843279	6.378801492
8	7.498952275	8.838629595	13.270774276
8	-2.703139147	6.081833308	0.461171845

8	-2.711120422	6.085798135	7.335642224
8	6.697648946	6.057837945	0.462987948
8	6.704435595	6.032763643	7.340613435
8	-7.431048376	14.223331895	0.491265226
8	-7.401148621	14.200600073	7.312286470
8	1.990976960	14.205974154	0.468924737
8	2.041760355	14.181258943	7.319867094
8	7.434555407	2.047940304	6.387239412
8	7.441402782	2.089922901	13.271370322
8	16.775361722	2.085980150	6.387897339
8	16.758181482	2.096845054	13.272420198
8	2.846626791	10.191731602	6.373355052
8	2.685169784	10.230172508	13.269635244
8	12.055431863	10.229234333	6.389833825
8	12.048440175	10.208325549	13.273897825
8	3.909376000	5.330839088	3.899548381
8	3.886423593	5.440147318	10.784768767
8	13.279398964	5.353392963	3.897546259
8	13.289145302	5.359279974	10.777441428
8	-0.787270326	13.468245861	3.892808441
8	-0.787546843	13.486829016	10.773481530
8	8.565862982	13.469880328	3.889761410
8	8.604562791	13.497082750	10.769353722
8	0.776537860	2.818220428	2.957494703
8	0.781281327	2.842047407	9.826132121
8	10.194370752	2.801100901	2.961127540
8	10.198771909	2.778290521	9.826039723
8	-3.901734067	10.932304605	2.957231349
8	-3.911358054	10.897709521	9.819978504
8	5.502194937	10.982011593	2.929788253
8	5.501025833	10.919818288	9.844643470
8	2.802441351	0.704147497	3.895411905
8	2.780840764	0.765972256	10.714166614
8	12.184300354	0.693448919	3.894184095
8	12.179974651	0.697845134	10.777413524
8	-1.869712884	8.860050959	3.892389309
8	-1.874558213	8.856261602	10.773257130
8	7.444702551	8.823067719	3.905707901
8	7.501649945	8.840950240	10.778022528
8	1.873783768	7.438497269	2.972283785
8	1.907317255	7.476410038	9.817288440
8	11.288377289	7.450395899	2.956208306
8	11.273555323	7.437888622	9.830607019
8	-2.818055394	15.559104742	2.968125047
8	-2.789193090	15.589609794	9.809303584
8	6.534464615	15.560627704	2.970850625
8	6.611613664	15.611494964	9.811767356
8	7.431161425	2.050406536	3.898822183
8	7.438738597	2.089905692	10.779664814
8	16.770922704	2.087280414	3.897627523
8	16.749813345	2.099053323	10.776270391
8	2.855704705	10.187948873	3.919864513
8	2.685802528	10.228334087	10.782863152
8	12.050831823	10.233522348	3.896070852
8	12.043432285	10.212250759	10.773574416
8	-2.705028503	6.085706068	2.953072822
8	-2.694929141	6.079353550	9.827831575
8	6.709469718	6.032136254	2.951848556
8	6.705928199	6.054534655	9.829557623
8	-7.387146848	14.190148600	2.979551584
8	-7.419108390	14.215599454	9.800699231
8	2.042670799	14.180532979	2.965750710
8	1.996455031	14.203241905	9.817347016
9	18.761402812	0.017772909	1.742836816
9	18.759239437	0.017982470	8.552774037
9	0.000016929	16.280299798	1.730189332
9	0.000517931	16.278129318	8.569025847
9	-4.699737055	8.152092037	1.711997749
9	-4.699643320	8.151087790	8.590815058
9	4.714224225	8.166403057	1.784552077

9	4.713037272	8.162593140	8.538394290
9	9.362171451	16.281789382	5.134951596
9	-0.021644768	-0.001938490	12.015791884
9	0.009403638	16.246292022	5.137233836
9	0.002548070	16.278929019	12.022559957
9	14.076677297	8.144663117	5.143429081
9	-4.699635268	8.151922356	12.020778806
9	4.673684338	8.002370081	5.149652702
9	4.707692287	8.163216738	12.027868944

EXAFS spectrum of Durango apatite measured on FAME-UHD

2.5000	-0.096252
2.5500	-0.045720
2.6000	-0.0034365
2.6500	0.036065
2.7000	0.071844
2.7500	0.098624
2.8000	0.11226
2.8500	0.11935
2.9000	0.11174
2.9500	0.095042
3.0000	0.083590
3.0500	0.065356
3.1000	0.045377
3.1500	0.039627
3.2000	0.035188
3.2500	0.035926
3.3000	0.034318
3.3500	0.037123
3.4000	0.035754
3.4500	0.030352
3.5000	0.020697
3.5500	0.0049137
3.6000	-0.0078926
3.6500	-0.023631
3.7000	-0.039874
3.7500	-0.045355
3.8000	-0.045444
3.8500	-0.046777
3.9000	-0.047993
3.9500	-0.048546
4.0000	-0.046454
4.0500	-0.044406
4.1000	-0.043535
4.1500	-0.034342
4.2000	-0.018100
4.2500	-0.0012503
4.3000	0.010947
4.3500	0.020293
4.4000	0.025090
4.4500	0.028016
4.5000	0.027668
4.5500	0.024052
4.6000	0.021243
4.6500	0.013914
4.7000	0.0072647
4.7500	0.0038517
4.8000	-8.9974e-05
4.8500	-0.0036865
4.9000	-0.0050456
4.9500	-0.0045652
5.0000	-0.0058546
5.0500	-0.0023051
5.1000	0.0088106
5.1500	0.016375
5.2000	0.022008
5.2500	0.023962
5.3000	0.017427
5.3500	0.015011
5.4000	0.011797

5.4500 0.0018258
5.5000 5.1639e-05
5.5500 -0.0030299
5.6000 -0.011271
5.6500 -0.015343
5.7000 -0.020243
5.7500 -0.026203
5.8000 -0.026683
5.8500 -0.017742
5.9000 -0.014807
5.9500 -0.017340
6.0000 -0.021476
6.0500 -0.011898
6.1000 -0.0012348
6.1500 0.0075337
6.2000 0.0096617
6.2500 0.019258
6.3000 0.023097
6.3500 0.015667
6.4000 0.018029
6.4500 0.016242
6.5000 0.0086194
6.5500 0.0081524
6.6000 0.0011532
6.6500 -0.0093705
6.7000 -0.0061468
6.7500 -0.0050710
6.8000 -0.0030558
6.8500 -0.0053557
6.9000 0.0021153
6.9500 0.0026021
7.0000 -0.00028372
7.0500 0.0029845
7.1000 0.0020452
7.1500 0.0035960
7.2000 -0.0010280
7.2500 -0.0035058
7.3000 -0.0051100
7.3500 -0.0060543
7.4000 -0.0057650
7.4500 -0.0072361
7.5000 -0.0072989
7.5500 -0.0054153
7.6000 -0.0040626
7.6500 -0.0026145
7.7000 0.0024358
7.7500 0.0060414
7.8000 0.0067560
7.8500 0.0078724
7.9000 0.0044022
7.9500 0.0012902
8.0000 0.0038620
8.0500 0.0040236
8.1000 0.0032208
8.1500 0.0029432
8.2000 -0.0010131
8.2500 -0.0032790
8.3000 -0.0051100
8.3500 -0.0040637
8.4000 -0.0012968
8.4500 -0.00019127
8.5000 -0.00017960
8.5500 0.0011338
8.6000 -0.00042640
8.6500 -0.0012367
8.7000 0.00095895
8.7500 0.0028951
8.8000 0.00047861
8.8500 -0.00094246
8.9000 0.0017463

8.9500 0.0019876
9.0000 -0.0026151
9.0500 -0.0035535
9.1000 -0.0022670
9.1500 -0.0026673
9.2000 -0.0052786
9.2500 -0.0021929
9.3000 0.0017483
9.3500 0.0022302
9.4000 0.0022291
9.4500 0.0017168
9.5000 0.0015086
9.5500 0.0024608
9.6000 0.0011194
9.6500 0.0022258
9.7000 0.0050673
9.7500 0.0036302
9.8000 -0.0010479
9.8500 -0.0029347
9.9000 -0.00011018
9.9500 0.00049115
10.000 -0.0014126
10.050 -0.0014208
10.100 -0.0023414
10.150 -0.0028011
10.200 -0.0018214
10.250 -0.0019143
10.300 -0.0014082
10.350 -0.0014382
10.400 -5.2058e-05

EXAFS spectrum of Durango apatite measured on ID24

2.5000 -0.086069
2.5500 -0.051740
2.6000 -0.012006
2.6500 0.024093
2.7000 0.056118
2.7500 0.078940
2.8000 0.096976
2.8500 0.10708
2.9000 0.10992
2.9500 0.10263
3.0000 0.089178
3.0500 0.075551
3.1000 0.055826
3.1500 0.040439
3.2000 0.026840
3.2500 0.020297
3.3000 0.016386
3.3500 0.013639
3.4000 0.012592
3.4500 0.0088105
3.5000 0.0028457
3.5500 -0.0044123
3.6000 -0.014477
3.6500 -0.025397
3.7000 -0.034593
3.7500 -0.041820
3.8000 -0.046904
3.8500 -0.048100
3.9000 -0.047524
3.9500 -0.046103
4.0000 -0.045066
4.0500 -0.041537
4.1000 -0.036602
4.1500 -0.028246
4.2000 -0.016233
4.2500 -0.0036438
4.3000 0.0067434
4.3500 0.016268

4.4000 0.023809
4.4500 0.026827
4.5000 0.027379
4.5500 0.026702
4.6000 0.023845
4.6500 0.019496
4.7000 0.015085
4.7500 0.011527
4.8000 0.0080304
4.8500 0.0043769
4.9000 0.0016301
4.9500 0.00064078
5.0000 0.0012807
5.0500 0.0015357
5.1000 0.0033889
5.1500 0.0071302
5.2000 0.0097869
5.2500 0.011063
5.3000 0.010419
5.3500 0.0079620
5.4000 0.0030466
5.4500 -0.0018494
5.5000 -0.0044753
5.5500 -0.0054697
5.6000 -0.0069915
5.6500 -0.010588
5.7000 -0.014915
5.7500 -0.017689
5.8000 -0.016737
5.8500 -0.014128
5.9000 -0.013137
5.9500 -0.014478
6.0000 -0.012896
6.0500 -0.0097491
6.1000 -0.0046882
6.1500 0.0020940
6.2000 0.0076636
6.2500 0.010890
6.3000 0.013035
6.3500 0.014282
6.4000 0.014088
6.4500 0.011869
6.5000 0.0094003
6.5500 0.0073621
6.6000 0.0035624
6.6500 -0.0018255
6.7000 -0.0050688
6.7500 -0.0042296
6.8000 -0.0026977
6.8500 -0.0021917
6.9000 -0.0021680
6.9500 -0.0016233
7.0000 -0.00099464
7.0500 -0.00016423
7.1000 0.0011613
7.1500 0.0010782
7.2000 0.00058766
7.2500 -0.00070671
7.3000 -0.0031976
7.3500 -0.0034309
7.4000 -0.0036845
7.4500 -0.0046083
7.5000 -0.0031918
7.5500 -0.0016818
7.6000 -0.00030985
7.6500 -0.00055444
7.7000 0.00017722
7.7500 0.0022999
7.8000 0.0033400
7.8500 0.0042637

7.9000 0.0034286
7.9500 0.0034087
8.0000 0.0028021
8.0500 0.0020395
8.1000 0.0013490
8.1500 0.0011640
8.2000 -0.0011175
8.2500 -0.0020062
8.3000 -0.0020420
8.3500 -0.0013772
8.4000 -0.0013329
8.4500 -0.00081975
8.5000 -0.00068989
8.5500 -0.00039273
8.6000 -0.00024817
8.6500 -0.00027684
8.7000 -0.00046088
8.7500 -0.00020332
8.8000 0.00028250
8.8500 -0.00051243
8.9000 -0.00058734
8.9500 -0.0015527
9.0000 -0.0023425
9.0500 -0.0020482
9.1000 -0.0013285
9.1500 -0.0011026
9.2000 -0.0022643
9.2500 -0.0012793
9.3000 -0.00078079
9.3500 -0.00012330
9.4000 0.00090597
9.4500 0.0015535
9.5000 0.0012893
9.5500 0.0018401
9.6000 0.0022821
9.6500 0.0023457
9.7000 0.0028299
9.7500 0.0029452
9.8000 0.0026821
9.8500 0.0019583
9.9000 0.00099696
9.9500 4.2563e-06
10.000 0.00015271
10.050 -0.00017758
10.100 0.00048826
10.150 -0.00036098
10.200 -0.0021954
10.250 -0.0018545
10.300 -0.0021366
10.350 -0.0028273
10.400 -0.0024002

EXAFS spectrum of Imilchil apatite measured on BM20

2.5000 -0.087850
2.5500 -0.052709
2.6000 -0.012356
2.6500 0.030397
2.7000 0.067925
2.7500 0.096936
2.8000 0.11775
2.8500 0.12653
2.9000 0.12397
2.9500 0.11306
3.0000 0.094036
3.0500 0.070214
3.1000 0.048560
3.1500 0.034130
3.2000 0.022611
3.2500 0.013894
3.3000 0.0093002
3.3500 0.0088011

3.4000 0.0083194
3.4500 0.0059332
3.5000 0.0020222
3.5500 -0.0078052
3.6000 -0.019385
3.6500 -0.029284
3.7000 -0.038348
3.7500 -0.043864
3.8000 -0.045512
3.8500 -0.047336
3.9000 -0.049145
3.9500 -0.047538
4.0000 -0.045699
4.0500 -0.044039
4.1000 -0.037423
4.1500 -0.028534
4.2000 -0.017519
4.2500 -0.0029764
4.3000 0.0081335
4.3500 0.015620
4.4000 0.020620
4.4500 0.023665
4.5000 0.024272
4.5500 0.023245
4.6000 0.020623
4.6500 0.015378
4.7000 0.011366
4.7500 0.0082097
4.8000 0.0042483
4.8500 0.0035787
4.9000 0.0048005
4.9500 0.0045643
5.0000 0.0055831
5.0500 0.0078807
5.1000 0.010061
5.1500 0.012135
5.2000 0.014083
5.2500 0.013446
5.3000 0.011191
5.3500 0.0086495
5.4000 0.0033359
5.4500 -0.0024576
5.5000 -0.0061751
5.5500 -0.0094093
5.6000 -0.012237
5.6500 -0.014470
5.7000 -0.016747
5.7500 -0.018297
5.8000 -0.016915
5.8500 -0.013092
5.9000 -0.011263
5.9500 -0.012170
6.0000 -0.011168
6.0500 -0.0069276
6.1000 -0.0015312
6.1500 0.0030855
6.2000 0.0067398
6.2500 0.0096260
6.3000 0.011141
6.3500 0.011768
6.4000 0.011911
6.4500 0.010665
6.5000 0.0085288
6.5500 0.0057420
6.6000 0.0026985
6.6500 -0.0010908
6.7000 -0.0037000
6.7500 -0.0039228
6.8000 -0.0039742
6.8500 -0.0031791
6.9000 -0.0016465
6.9500 -0.0015549
7.0000 -0.0017399
7.0500 -0.0011457
7.1000 -0.00039838

7.1500 -0.00054303
7.2000 -0.00080400
7.2500 -0.00055174
7.3000 -0.0012504
7.3500 -0.0031494
7.4000 -0.0042145
7.4500 -0.0035135
7.5000 -0.0015187
7.5500 -5.6599e-05
7.6000 0.00069428
7.6500 0.0017456
7.7000 0.0030173
7.7500 0.0034498
7.8000 0.0021659
7.8500 0.0018294
7.9000 0.0024114
7.9500 0.0020550
8.0000 0.0015824
8.0500 0.00080422
8.1000 0.00037195
8.1500 0.00084576
8.2000 0.00025243
8.2500 -0.0010086
8.3000 -9.7989e-06
8.3500 0.00072112
8.4000 0.00025463
8.4500 0.00077665
8.5000 0.00049537
8.5500 -0.00094348
8.6000 -0.00087168
8.6500 0.0012149
8.7000 0.0012429
8.7500 -0.00055663
8.8000 -0.0012447
8.8500 -0.0013341
8.9000 -0.0016017
8.9500 -0.0023305
9.0000 -0.0024625
9.0500 -0.0020448
9.1000 -0.0019730
9.1500 -0.0011214
9.2000 -0.00019757
9.2500 -0.00077469
9.3000 -0.0010906
9.3500 -0.00074049
9.4000 -0.00016591
9.4500 2.8602e-06
9.5000 -1.6476e-05
9.5500 0.00043085
9.6000 0.00096817
9.6500 0.0012670
9.7000 0.00094514
9.7500 0.0011273
9.8000 0.0016746
9.8500 0.0013154
9.9000 0.00067551
9.9500 0.0010378
10.000 0.0019301
10.050 0.0019060
10.100 0.00066569
10.150 -8.8946e-05
10.200 -0.00021102
10.250 -0.00013918
10.300 0.00053326
10.350 0.00088069
10.400 0.00074169